Supplementary material for: *Finding the most efficient way to remove residual copper from steel scrap*.

Katrin E. Daehn, André Cabrera Serrenho, Julian Allwood.

University of Cambridge, Department of Engineering
Trumpington Street, Cambridge, UK, CB2 1PZ

Contents

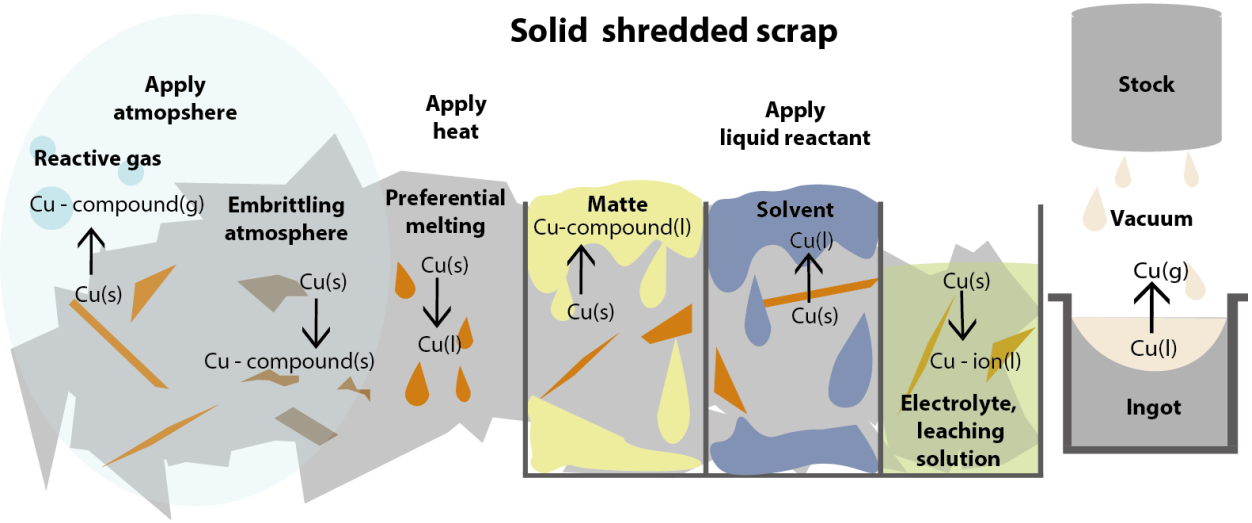

Figure S-1: Possible phase distributions for removing copper from shredded steel scrap.

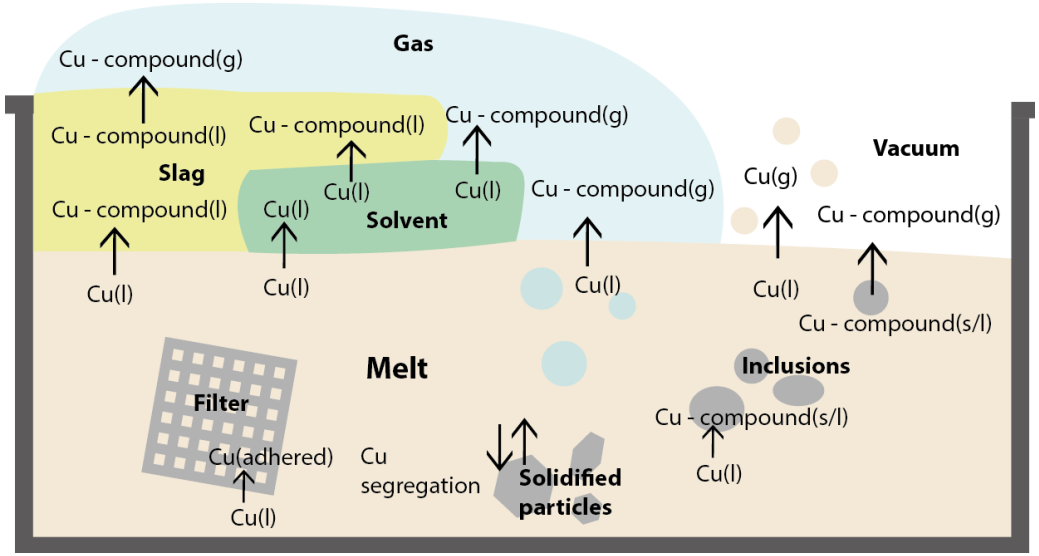

Figure S-2: Possible phase distributions for removing copper from the steel melt.

Table S-1: Catalogue of studies for improved shredding and magnetic separation.

Author	Year	Title	Alternative processing	Main results
Newell [1]	1996	Production of low copper residual shredded steel scrap	Describes several strategies for the scrap processor to employ: careful control of the input materials, hand-picking, and higher-density shredding.	Density has a large effect on the amount of copper removed. Higher density means lower copper residual range. Increasing the density from 65 lb/cubic ft to 85 lb/cubic ft adds $2-$4/ton (due to additional electrical power, more time in the shredder and more labor), and reduces Cu to 0.09 to 0.12 wt%.
Katayama, Sano, Sasabe, Matsuoka [2]	1997	Research activities in Japan on removal of residual elements from ferrous scrap	Cryogenic shredding at -100 to -200ºC for brittle fracture instead of plastic shearing Reiterating shredding and magnetic separation	95% of copper can be removed, but costs of this process are prohibitive and there has been little further development of this idea. 0.15wt% Cu can be achieved with three passes through the shredding and magnetic separation
Newell [3]	2017	The true value of shredded steel when used in EAF steel production	High-density shredding	Shredding normal scrap (70 lb/cubic ft) to 10-15 lb/cubic ft higher density will reduce the copper content by about 0.1 points.

Table S-2: Catalogue of studies for density separation/isolating a copper-rich fraction.

Author	Year	Title	Alternative processing	Main results
Aboussouan et al. [4]	1999	Steel scrap fragmentation by shredders	Use sieve meshes to separate scrap stream by different sizes.	Most copper was found between mesh sizes 20 and 60 mm. Simply sieving and separating fraction for other sizes would reduce the initial copper by up to 90%. However, a use for this large fraction of high-copper scrap is required.
Shulman [5]	2011	US Patent: Method for bulk sorting of shredded scrap metal	A stream of shredded scrap is sorted by copper content using bulk composition analysis, such as neutron activation	Author claims this technique could generate grades of scrap with specific copper concentration values, such as 0.2 and 0.1wt% Cu.
Russo [6]	2014	Quality control of scrap and chemical analysis needs at ArcelorMittal	Use neutron activation analysis (by Gamma Tech) to measure scrap copper content before it is charged and melted.	Statistical analysis of the composition of steel melts can provide overall trends on copper concentration, but it is difficult to trace to specific scrap supplies. Bulk composition analysis can be used for real-time control over copper concentration.
Newell [3]	2017	The true value of shredded steel when used in EAF steel production	Trommel sorting	Engine blocks, powder metallurgy products fall through screen while sheet passes to produce scrap with 0.12-0.15 wt% Cu.
SICON [7]	2018	SICON PrimeScrap: low-copper shredded scrap	Scrap is transported from a vibrating feeder to a chute, where it is accelerated to 20 ft/s. A head drum with a magnet system ejects copper-rich pieces.	Copper “meatballs” are ejected. 75% of material is clean ferrous scrap, and the copper-rich fraction (25%) goes to further sorting/handpicking.
STEINERT [8]	2018	SteelMaster: Separate your heavy ferrous parts	Combines magnetic field forces and ballistic effects to concentrate copper impurities in 20-30% of the overall mass stream	Less magnetically permeable material is separated with ballistic forces. 110t scrap/hour.
Shattuck and Ramsdell [9]	2018	The case for ballistic metal separators	A ballistic separator uses a fast belt, high magnetic attraction and a charged trajectory method.	A ballistic separator can ensure 0.16 to 0.17wt%Cu. Reports that it offers low operating costs, requires no air and uses very little electricity. Process rates of 100 t/hr.

Table S-3: Catalogue of studies for applying a reactive gas to solid scrap.

Author	Year	Title	T (ºC)	Main results	Information provided by
Hartman, Oden and Davis [10]	1994		650 to 800	Reported the deposition of copper on iron when oxide film is not formed. The rate of copper removal is a function of time, and an increase in temperature from 650 to 800ºC reduces the amount of copper deposited on iron. Recommended 800ºC to ensure a good oxide bond and obtain reasonable vapor pressure for copper chloride volatilization.	Tee and Fray (2006)
Hartman, Williamson and Davis [11]	1996		800	Used 11% HCl and 89% air at 800ºC. The condensed products, copper and zinc chlorides, were treated by solvent extraction and electrowinning to obtain copper and zinc. 74% of copper was removed from 3.5 kg of scrap in 90 minutes.	Savov and Janke
Matsumaru, Susa and Nagata [12]	1996	Removal of copper from iron-based scraps by O_2-Cl_2 gas mixtures	827	Determined evaporation rate limited by the transport of chlorides across the boundary layer. Using thermodynamic and kinetic considerations proposed the optimal condition of 827ºC and O_2-10%Cl_2 gas. In Japanese.	
Katayama, Sano and Sasabe [2]	1997	Research activities on residual element removal in Japan		Reported chloridization and vaporization of copper as a feasible technique, but noted practical application would call for protection of the apparatus against corrosion and the treatment of waste gas.	
Tee and Fray [13]	1999	Removing impurities from steel scrap using air and chlorine mixtures	800	Presented process conditions for large scale dezincing of steel scrap with chlorination, with an economic evaluation and market analysis. Discussed how copper could also be chlorinated.	
Tee and Fray [14]	2004	Reaction of zinc, copper and iron in air and chlorine mixtures	800	Showed copper can be separated from iron via chlorination, forming volatile copper chloride. All copper chlorinated in 10 min. However, if iron did not have a cohesive oxide film, copper could deposit onto iron, and thus not separate.	
Tee and Fray [15]	2006	Separation of copper from steel	800	Recommended optimum conditions of air/chlorine ratio of 10:1, flow rate: 400/40 cm^3/min and 800ºC with an initial oxidizing treatment to form the protective layer of iron oxide. Experiments were performed with Fe and windings of copper wire from 60wt%, 13wt% and 1wt%, the latter of which could be reduced to 0.05wt% in 10 minutes.	

Table S-4: Catalogue of studies for preferential melting.

Author	Year	Title	T (ºC)	Set up	Main results
Brown and Block [16]	1968	Copper removal form steel scrap by thermal treatment, U.S. Bureau of Mines Report No. 7218	600 to 1150	Furnace in various oxidizing, reducing and neutral atmospheres. Recommended a traveling grate system over a rotary kiln.	Treated automotive scrap, but copper was not successfully removed with raised temperatures. Liquation varied considerably and the surface area between copper and iron must be kept to a minimum to prevent wetting.
Elger [17]	1968	Removal of non-ferrous metals from synthetic automobile scrap on heating in a rotary kiln	450 to 1150	Rotary kiln under oxidizing and reducing atmosphere	Copper was most successfully removed when it was embrittled. Otherwise, copper wetted the steel with heavy oxidation. High metal loss, high fuel cost and excessive refractory wear were noted.
Leak, Fine and Dolezal [18]	1973	Separation of copper from scrap by preferential melting	1150 to 1250	Various combinations of sweating media and pre-coatings	Achieved ~0.15wt% Cu with sodium silicate pre-coating in $BaCl_2$ molten salt bath.
Katayama, Sano, Sasabe, Matsuoka [2]	1997	Research activities in Japan on removal of residual elements from ferrous scrap	1100	Measured work of adhesion of liquid copper on various steel oxide films	The flow-off of copper droplets from the steel surface was investigated as a function of oxygen partial pressure. Copper easily flows down magnetite and iron-silica surfaces, but the adherence between copper droplets and wüstite is high.
Freuhan and Cramb [19]	1991	Copper removal from steel using sulfur matte			Reviewed preferential melting as unsuccessful due to copper wetting solid iron.
Savov, Volkova, Janke [20]	2003	Copper and tin in steel scrap recycling			Reviewed preferential melting and concluded poor separation due to liquid copper entrapping in cavities, and disadvantages of iron oxidation and high fuel costs, unless integrated into scrap pre-heating.

Table S-5: Catalogue of studies for applying solvent extraction to solid scrap.

Author	Year	Title	T (°C)	Set up	Main results
Iwase, Masanori, Tokinori, Kenji [21]	1991	Feasibility study for the removal of copper from solid ferrous scrap	745	Al bath	Pilot study. Claimed scrap is clean of copper contamination after immersion for 5 to 10 minutes.
Iwase, Ohshita [22]	1994	Further studies of the removal of copper from solid ferrous scrap	690 to 950	2-step Al bath process	Proposed solution to Al-Cu alloy adhering to scrap with 2-step process
Iwase [23]	1996	Refining of solid ferrous scrap intermingled with copper by using molten aluminum	690 to 950	2-step Al bath process, with vibration	Intermingled scrap was immersed for 5 to 30 minutes into an Al-Cu bath, followed by mechanical shaking and immersed in a pure Al bath to achieve as low as 0.04wt% Cu.
Katayama, Sano, Sasabe, Matsuoka [2]	1997	Research activities in Japan on removal of residual elements from ferrous scrap			Reviewed Al extraction, noting Al is the most viable solvent as it is easy to handle and copper can be readily separated from Al

Table S-6: Catalogue of studies for applying matte extraction to solid scrap.

Author	Year	Title	Slag system	T(°C)	Main results
Jimbo and Freuhan [24]	1988	The refining of copper from ferrous scrap	FeS - (19-25wt%) Na_2S	800, 900, 1000	Experiments on 100g of scrap confirmed that the reaction is more favorable in the solid state. L~500. Planned a larger scale experiment.
Cramb and Fruehan [19]	1991	Copper removal from steel using sulfur matte	FeS – 18wt% Na_2S	1000	10 kg matte/tonne scrap to decrease from 0.4wt% to 0.1wt%. Demonstrated process in a rotary kiln at 1-10RPM with 100 kg scrap. The treated scrap needed desulfurizing because matte adhered to the scrap. One suggestion was to use hot acid, but hydrogen sulphide would be produced as a result.

Table S-7: Catalogue of studies for oxygen embrittlement.

Author	Year	Title	T (C)	Atmosphere	Set up	Main results
Leary [25]	1965	Removal of copper from copper-clad steel by oxidation	650 to 1040	Various flow rates of oxidizing gas	Horizontal muffled furnace, treatments of 15 to 120 minutes	All copper oxidized and the copper oxide scale could be easily separated from underlying steel during cooling, while steel oxidation was limited. Light-gage copper coatings could be removed in an incineration process.
Brown and Block [16]	1968	Copper removal from steel scrap by thermal treatment	800 to 900	Oxidizing, neutral and reducing	Furnace treatment followed by 15 minutes of tumbling	Major compounds in the scale were 1-10% $CuO•Fe_2O_3$ and $Cu_2O•Fe_2O_3$, CuO, Cu_2O, FeO, Fe_2O_3, and Fe_3O_4. Scale formation was more effective with insulated wire than bare, possibly due to the presence of lead. Experiments with a lead wire showed lead oxide is likely involved in copper's embrittlement. Tried various chemical pretreatments and $Na_2Si_4O_9$ may embrittle copper.
Elger [17]	1968	Removal of nonferrous metals from synthetic automobile scrap on heating in a rotary kiln	450 to 1160	Oxidizing, neutral and reducing	Rotary kiln	In some cases, copper wiring was embrittled and mechanically removed by fragmentation. Authors thought the insulation of the wire might have embrittled the copper. In an oxidizing atmosphere, the percent of copper removed increased with temperature.
Herter [26]	1985	Method for preparing a low residual alloy steel charge from scrap metal	930 to 1040	Oxidizing, neutral to reducing	Rotary kiln	Scrap enters the kiln in the oxidizing condition, then the atmosphere changes to neutral and reducing as the temperature increases to form a brittle scale of external impurities. Rates of 50% copper removal were reported.
Cho and Fan [27]	2004	A new approach for the removal of copper from solid ferrous scrap	400 to 700	Oxidizing	Oxidizing treatment for 4 to 6 hours with thermal cycling, followed by mechanical impacting and a fluxing process from 1000 to 1200ºC	Over 90% of copper can be removed from scrap containing initially 3 to 5 wt% by utilizing the preferential oxidation of copper.

Table S-8: Catalogue of studies for leaching.

Authors	Year	Title	Leach solution	T (ºC)	Main results
Staker, Chindgren, Dean [28]	1971	Improved cupric ammonium carbonate leaching of copper scrap	Ammonium carbonate	25 to 40	Showed leaching with ammonium carbonate to be very effective. Used entrained air bubbles to increase the copper dissolution rate to 1.5 g/in^2/hr. Also proposed using powdered sulfur to precipitate copper from solution.
Oden, Adams and Fugate [29]	1972	Reducing copper and tin impurities in ferrous scrap recovered from incinerated municipal refuse	Ammonium carbonate	25	Achieved 0.1-inch penetration per 24-hour period, sufficient to dissolve thickest copper pieces and reduce from 0.6 to 0.5wt% Cu to 0.1 to 0.2wt% Cu. Suggested a tumbling reactor, with vigorous aeration and excess ammonia.
Chin [30]	1977	Electrochemical extraction of copper from scrap steel	Ammonium sulfate and carbonate, pyrophosphate, alkaline cynaide	25	Tested four electrolytes in an electrochemical packed bed cell. Achieved less than 0.06% Cu with alkaline cyanide, but did not yet achieve copper deposition on the cathode.
Majima, Nigo, Hirato, Awakura and Iwai [31]	1993		Ammonium sulfate		Leaching speed increased with increasing NH_3 up to 7 kmol/m^3 and optimum $(NH_4)SO_4$ concentration existed corresponding to NH_3 concentration. Referenced by Konishi.
Zhou, Shinme and Anezaki [32]	1995	Removal of copper from ferrous scrap with ammonia leaching method	Ammonium carbonate	40	Leaching speed increased with increasing Cu(II) concentration, O2 gas flow rate and bath temperature. Tested with 200-liter tank and argued ammonia leaching with air injection in a closed circuit system is effective to remove copper from automobile scrap.
Meng and Han [33]	1996	The principles and applications of ammonia leaching of metals - a review			Reviews the thermodynamics of the Cu-NH_3-H_2O system, as well as the kinetics of copper dissolution. When air is the oxidant, oxygen and ammonia determine the overall rate.
Katayama, Sano, Sasabe [2]	1997	Research activities on residual element removal in Japan	Ammonium, concentrated nitric acid, sulfuric acid		Reviewed several possible leachants and concluded an amine ion solution with oxygen blowing dissolved copper with the greatest stability and relatively high rate. Noted motors must be heated to remove enamel before dissolving copper.

Koyama, Tanaka, Lee [34]	2006	Copper leaching behavior from wasted printed circuit board in ammoniacal alkaline solution	Ammonium alkaline solution	25 to 55	Studied leaching rate of copper from crushed PCB's to understand feasibility of electrowinning set-up, with $Cu(NH_3)_4$ as the oxidizing agent instead of oxygen. 200 RPM stirring, temperature effects insignificant, used 0.3 kmol/m^3 $CuSO_4$, 5 kmol/m^3 NH_3, 1 kmol/m^3 $(NH_4)_2SO_4$ solution to achieve 80% leaching from 3.5 mm diameter particles in 4 hours.
Lim, Kwon, Lee, Yoo [35]	2013	The ammonia leaching of alloy produced from waste printed circuit boards smelting process		30	Suggested 2 kmol/m^3 NH_4Cl and 5 kmol/m^3 NH_3 with 0.1 kmol/m^3 $CuCl_2$ at 200 RPM and 30ºC for 3 kg/m^2hr leaching rate.
Konishi, Bitoh, Ono, Oishi, Koyama, Tanaka [36]	2014	Behavior of copper dissolution in an ammonia solution containing ammonium chloride or sulfate	Ammonium chloride and ammonium sulfate solutions	25 to 80	Found ammonium chloride solutions to be superior to ammonium sulfate solutions. Reported relationship between stirring speed and leaching rate. Achieved maximum leaching speed of 3.98 kg/m^2hr at 80ºC with 600 RPM stirring with 4kmol/m^3 NH_3 and 1 kmol/m^3 NH_4Cl with 0.5 kmol/m^3 Cu(II).
Sun, Xiao, Sietsma, Agterhuis, Yang [37]	2015	A cleaner process for selective recovery of valuable metals from electronic waste of complex mixtures of end-of-life electronic products	Ammonium carbonate, sulfuric acid and salt-aluminum chloride solutions	20 (ammonia solutions), 80 (other)	Describes a two-step hydrometallurgy process to extract metals from e-waste. Leached copper with an ammonia-based leachant, then proved electrodeposition from an ammonium sulfate solution containing 51 g/l Cu with a current efficiency of 90%. The cell design is very important for achieving a high current efficiency.
Ghosh, Ghosh, Parhi, Mukherjee, Mishra [38]	2015	Waste Printed Circuit Boards recycling: an extensive assessment of current status			Reviewed hydrometallurgical routes for copper extraction and concluded ammonium leaching to be superior for selectivity. Reported that the effect of temperature on leaching rate is insignificant, but the concentration of the Cu(II)-amine complex enhances leaching rate, while Cu(I)-amine complex depresses it.
Rudnik [39]	2017	Application of ammoniacal solutions for leaching and electrochemical dissolution of metals from alloys produced from low-grade e-scrap	Sulfate, chloride and carbonate ammonium solutions	20	Anodically dissolving the metals was achieved, but the cathodic current efficiency of depositing of copper was low, below 1%.

Table S-9: Catalogue of studies for distillation.

Authors	Year	Title	Pressure regime /atmosphere	T (ºC)	Main result	Information provided by
Gill, Inveson, Wesley-Austin [40]	1959	The behavior of various elements in vacuum steelmaking	vacuum		0.32 to 0.01% in 90 min from 0.1 kg of steel, A/V=50m^{-1}.	Data from Harris
Olette [41]	1961	Vacuum distillation of minor elements from liquid ferrous alloys	vacuum		0.12 to 0.001% in 40 min from 0.5 kg Fe, A/V=10m^{-1}. Defined relative volatility.	Data from Harris
Ward [42]	1963	Evaporative losses during vacuum induction melting	vacuum		1.0 to 0.1% in 120 min from 12 kg Fe, A/V=8m^{-1}.	Data from Harris
Turkdogan, Grieveson, Darken [43]	1963	Enhancement of diffusion-limited rates of vaporization of metals	atmospheric		Showed that the rate of vaporization of metals in a stream of neutral atmosphere can be increased by increasing the partial pressure of a reacting gas, until a critical value, at which point a surface film forms.	
Fischer and Derenbach [44]	1964	Contribution to the question of evaporation in melts of iron alloys in a vacuum: Part 1. Theoretical investigations on binary alloys of iron with arsenic, manganese, copper and tin	vacuum	1627	0.17 to <0.001% in <60 min from 0.03 kg Fe, A/V=50m^{-1}.	Data from Harris
Smith and Ward [45]	1966	The evaporation of liquid iron alloys under vacuum	vacuum, ~0.1 Pa	1700 to 1760	0.55 to 0.1% in 0.2 min from 0.001 kg Fe, A/V=500m^{-1}. Rate of evaporation of copper from levitated droplets was 50-70% of the theoretical value, suggesting liquid diffusion of copper is a rate-limiting step.	
Ohno and Ishida [46]	1968	Rate of evaporation of manganese, copper, tin, chromium and sulphur from molten iron under vacuum	vacuum	1600	1.0 to 0.1% in 15 min from 0.15 kg Fe, A/V=60m^{-1}.	Only abstract found. Data from Harris
Fischer, Janke and Stahlschmidt [47]	1974	The evaporation of copper, manganese and chromium from melts of steel X5 Cr Ni 18 9 under reduced pressure	vacuum		1.9 to 0.1% in 50 min from 5 kg X5 Cr Ni 18 9 steel, A/V=11m^{-1}.	Data from Harris

Salomon De-Friedberg and Davenport [48]	1977	Vacuum removal of copper from melted steel scrap	vacuum		0.5 to 0.1% in 150 min from 26 kg steel, A/V=8m^{-1}.	Only abstract found. Data from Harris
Reiichi [49]	1977	Kinetics of evaporation of manganese, copper and sulphur from iron alloys in vacuum induction melting	vacuum	1415 to 1600	2.1 to 0.3% in 15 min from 0.15 kg steel, A/V=60m^{-1}.	Only abstract found. Data from Harris
Harris and Davenport [50]	1979	Pilot plant scale vacuum distillation of liquid steel to remove copper	vacuum, 3 to 20 Pa	1587 to 1617	2.0 to 0.1% in 180 min from 22 kg A36 steel, A/V=10m^{-1}. Found removal efficiency is reduced in large systems and concluded slow evaporation rates are caused by the presence of a thin surface film from air leakage.	
Yamamoto and Kato [51]	1980	The effect of surface movement on the evaporation rates of alloying elements from liquid iron under vacuum	vacuum		Both the evaporation step and the diffusion step through the liquid boundary layer are rate-controlling.	
Harris [52]	1980	Vacuum refining of molten steel, dissertation	vacuum, 3 to 2000 Pa	1507 to 1757	Developed a theoretical model to describe vacuum distillation and validated with experimental work. Found most favorable refining with high T, no surface films, low chamber pressure and induction mixing of the liquid.	
Morales [53]	1982	Alloying effect on vaporization rate of copper and tin from molten iron alloys		1800	C, Cr and Si were found to enhance the vaporization of Cu. K_{Cu} data point.	Only abstract accessed. Data from Ono-Nakazato, et al.
Harris and Davenport [54]	1982	Vacuum distillation of liquid metals: Part I. Theory and experimental study	3 to 20 Pa	1577 to 1777	Presented the kinetics of evaporating copper, as given in transport equations below. Confirmed with experimental results.	
Harris and Davenport [54]	1982	Vacuum distillation of liquid metals: Part II. Photographic study	5 to 25 Pa	1677	Photographs confirm the different vapor behavior as chamber pressure varies (bulk flow for low P, decaying to diffusive transport as the chamber pressure exceeds the melt vapor pressure) and the importance of surface cleanliness and avoiding condensate refluxing.	

Harris and Davenport [55]	1983	Vacuum purification of liquid metals: United States Patent	vacuum to atmospheric, with gas flow		Proposed using a scavenging gas to develop bulk flow at higher pressures, with a lifting gas to produce a spray.	
Harris [56]	1988	Numerical simulation of vacuum refining of liquid metal	vacuum to atmospheric		Proposed a mathematical model to simulate vacuum refining and applied it to the design constraints described in the "LSV" patent.	
Matsuo [57]	1988		2x10^4 Pa, with Ar flow		Applied argon-hydrogen and argon plasma flames under 2x10^4 Pa pressure at a laboratory scale. Found hot spot of plasma increased removal rate.	Matsuo, Maya, et al.
Nakajima, Okimura and Hirama [58]	1993	The report of committee on separation of circulative elements	0.2 to 200 Pa	1650	K_{Cu} data point.	Data found in Ono-Nakazato, et al.
Hino, Wang, Nakasaka, Ban-ya [59]	1994	Evaporation rate of zinc from liquid iron	High Ar flow rate		Identified that the issue with tramp element distillation from liquid iron is the evaporation of iron itself.	
Emi and Wijk [60]	1996	Residuals in steel products - impacts on properties and measures to minimize them			Concluded that removal of copper under vacuum is not practicable on a commercial scale	Warner
Matsuo, Maya, Nishi, Shinme, Ueno, Anezaki [61]	1996	Removal of copper and tin in molten iron with decarburization under reduced pressure	130 Pa	1650	Evaluated different oxidizing agents to generate fine CO bubbles in a 1-1.5 tonne vat and found SiO2 to be most effective.	
Lee and Harris [62]	1997	Characterization of the surface area of overflow droplets generated by a gas-lift pump under reduced pressure	Reduced, with gas flow		Used water-modelling experiments to characterize droplets under varying operating conditions to predict molten metal refining.	
Nishi, Fukagawa, Shinme, Matsuo [63]	1999	Removal of copper and tin in molten iron with combination of plasma heating and powder blowing decarburization under reduced pressure	130 to 650 Pa	1650	Used a combination of plasma heating and powder blowing decarburization in a 1-1.5 tonne vat. This could accelerate up to 4 times the removal rate.	
Zaitsev, Shelkova, Litvina, Shakhpazov, Mogutnov[64]	1999	An investigation of evaporation of liquid alloys of iron with copper		1167 to 1643	Determined thermodynamic characteristics of liquid alloys of iron with copper, including sublimation enthalpies.	

Ma, Savov and Janke [65]	1999	Chemical activities of the solute elements Cu and Sn in scrap-based iron melts		1600	Found evaporation of Cu and Sn can be enhanced by C and Si, but at quantities not practical in steelmaking. Recommended charging scrap with ferrosilicon grades, where high Si contents and C contents are desired.
Savov and Janke [66]	2000	Evaporation of Cu and Sn from induction-stirred iron-based melts treated at reduced pressure	1 to 100 Pa	1400 to 1600	Presented experimental results on 20 kg, A/V=6m^{-1} set up, quantifying the effects of chamber pressure, melt temperature, melt composition and stirring intensity on evaporation rate. Recommended pressures less than 10Pa, high melt temperatures and induction stirring.
Matsuo [67]	2000	Acceleration of copper and tin removal from molten steel by decarburization	130 Pa	1600 to 1700	Measured effective removal with different decarburization powders and found MgO>SiO_2 >O_2. The rate of decopperization was 1.5-3 times higher than without decarburization. Low oxygen was favorable as it is a surface-active element that can retard the reaction.
Ono-Nakazato, Taguchi, Seike, Usui [68]	2003	Effect of silicon and carbon on the evaporation rate of copper in molten iron	133 to 10^5 Pa with hydrogen flowing	1650 to 1700	Found C and So additions to increase the rate constant by 1.7 and 1.4 times respectively, and achieved a rate equivalent to chemical-reaction limiting at 133 Pa.
Taguchi, Ono-Nakazato, Usui [69]	2004	Enhancement of evaporation removal rate of copper in molten iron by the silicon and/or carbon addition	133 Pa	1650	Found the optimum composition for enhanced removal rate to be Fe-1.5Si-3C.
Zaitsev, Zaitseva, Mogutnov [70]	2004	Evaporation of copper from iron melts	10 Pa, 100 Pa and 0.1MPa, with and without gas blowing	1600	Modeling analysis of a 160-tonne vat with conditions ranging from an undisturbed surface, to high vacuum with high velocity gas stream blowing. Found blowing of the melt raises the rate of copper transfer to the gaseous phase by a factor of 1.7. Decarburizing with SiO_2 increased transfer by a factor of 2.2-2.6, and MgO by 2.8-3.1.
Zaitsev, Zaitseva, Mogutnov [71]	2004	Potentialities of simultaneous removal of tin and copper from molten iron through evaporation	100 Pa with gas blowing	1550	Modeling analysis of a 160-tonne vat with argon blowing found 0.01 to 0.6wt% tin additions did not affect the rate of evaporation of Cu.

Warner [72]	2004	Continuous oxygen steelmaking with copper, tin and zinc-contaminated scrap	250 Pa with desorption gas	1780	Kinetic analysis showed a typical RD-KTB vacuum pumping system could refine 0.6 Mtpa liquid scrap from 0.5% to 0.05% Cu.	
Blacha, Labaj [73]	2011	Temperature impact on copper evaporation from liquid iron	0.06 to 101 Pa	1650 to 1725	Measured activation energy of Cu evaporation under various conditions to determine the rate determining step. At low pressures the copper evaporation process is determined by mass transfer in the liquid phase.	Only abstract accessed
Labaj, Oleksiak, Siwiec [74]	2011	Study of copper removal from liquid iron	0.06 to 101 Pa	1377	Found liquid mass transfer and gaseous transfer to be rate-limiting between 10 and 100 Pa. Concluded vacuum distillation should be conducted at 10 Pa, for the maximum rate.	
Blacha, Labaj [75]	2012	Factors determining the rate of the process of metal bath components evaporation			Review paper on the effect of pressure, gaseous atmosphere, rate of bath mixing and melt composition on the rate of impurity evaporation.	
Jung and Kang [76]	2016	Evaporation mechanism of Cu from Liquid Fe containing C and S	Atmospheric, with 0-2 L/min Ar-4%H_2 and Ar-5%NH_3 gas mixture flowing	1600	Decopperization experiments were conducted with inert and reactive gas flows on Fe levitated droplets with C and S additions. S was found to accelerate the rate of Cu evaporation by forming CuS(g), but simultaneously decelerates by blocking evaporation sites. Found the rate constant of the CuS reaction.	
Jung and Kang [77]	2016	Simultaneous evaporation of Cu and Sn from liquid steel	Atmospheric, with 1L/min Ar-4%H2 gas mixture flowing	1600	Considering the mechanisms of Cu evaporation with C, S and Sn present in levitated droplets, found Cu evaporation could be increased at most to 2.2 times with 5%C and 0%S.	

Table S-10: Catalogue of studies for vacuum arc remelting.

Authors	Year	Title	Melt composition	T(ºC)	Melting rate (kg/hr)	Main results
Carlson and Schmidt [78]	1974	Paper presented at the 103rd Annual AIME Meeting	Automotive steel	1600 and 1750	1 to 4	Conducted experiments on the solute removal from automotive scrap steel using electron-beam-refining techniques
Andreini and Foster [79]	1974	Kinetics of solute removal during electron-beam and vacuum-arc melting	Fe-Cu	1600	1 to 4	Presented a model to describe the kinetics of dilute metallic-solute removal from molten alloys using electron beam or vacuum arc refining techniques. Applied model to refining of copper from automotive steel scrap and compared results to data in study above. Can predict the solute concentration in the final ingot for a given melt rate.
Scholz, Biebricher, Franz [80]		State of the art in VAR and ESR processes - a comparison	Fe-Cu	1600	540	Reviewed the methods and recent trends in process technology and provided rates of energy consumption.

Table S-11: Catalogue of studies for applying a reactive gas to the melt.

Authors	Year	Title	Main results
Turkdogan, Grieveson, Darken [81]	1963	Enhancement of diffusion-limited rates of vaporization of metals	Provides theory of reactive gas evaporation
Hidani, Takemura, Suzuki and Ono [82]	1996	Elimination of copper from molten steel by ammonia gas blowing	Blew NH3 gas onto molten steel under low pressure. Noted boiling, splashing and violent slopping and observed copper smoke from the surface. The mechanism of de-copperization was considered that gaseous CuH was produced and enhanced surface area.
Liansheng, Shiqi, Changxiang [83]	1999	Copper removal from molten steel by gasification	Ammonium salts or urea were added into 400g of molten steel under normal pressure at 1600C. Noted copper reduction of about 0.5 to 0.3 wt% Cu with about 0.5 g of NH_4C and $(NH_4)_2C_2O_4$.
Suzuki, Ono [84]	2000	Enhanced evaporation of copper by NH_3 gas blowing	Observed copper smoke from top-blowing NH_3 onto the melt and hypothesized that an unstable and volatile compound such as CuN_x or CuH was formed. Also noted the cooling effect due to the endothermal decomposition of NH_3. Also investigated the nitrogen solubility of the melt under application of the NH_3 gas.
Maruyama, Katayama, Momono, Tayu, Takenouchi [85]	1998	Evaporation rate of copper from molten iron by urea spraying under reduced pressure	Sprayed urea onto molten iron with 0.4wt% Cu at 1600ºC under reduced pressure. Noted splashing and reported the rate constant of copper evaporation as a function of pressure. Concluded that acceleration of copper evaporation by urea was mainly due to the evaporation of $Cu(N_3)_2$, which has a higher vapor pressure than metallic copper.
Li, Xiang, Cao, Ichise [86]	1998	Copper elimination from the molten steel by addition of hydronitrogens	Compounds of hydrogen and nitrogen (NH_4Cl and NH_2CONH_2) were added to the steel melt at normal pressure at 1600C. Noted copper reduction and that the technique was worthy of further study.
Li, Yu, Li, Li [87]	1999	A basic study of decopperization in molten steel by ammonium salt	Agents of NH_4Cl, $(NH_4)_2C_2O_4$ and $CO(NH_2)_2$ by feeding wires. NH_4Cl has the best result, efficiency of removing copper is 36%. The content of copper can be reduced from 0.6 to 0.3% with 4.5 kg/t agents
Jung, Kang, Seo, Park, Choi [76]	2014	Evaporation mechanism of Cu from liquid Fe containing C and S	Investigated the evaporation mechanism of Cu under argon and NH_3, but observed no appreciable difference in evaporation rate.

Table S-12: Catalogue of studies for injection.

Authors	Year	Title	Main results
Sasabe, Harada, Yamashita [88]	1996	Removal of copper from carbon saturated molten iron by using $FeCl_2$	Injected pulverized $FeCl_2$ with nitrogen gas into carbon-saturated molten iron. Iron chloride vaporized first, but noted decrease in copper content due to copper reacting with chlorine. Described with first order rate equation and estimated 18.5 kg of $FeCl_2$/t iron would be required to reduce Cu from 0.5 to 0.1wt%.

Table S-13: Catalogue of studies for solidification segregation.

Authors	Year	Title	Melt composition	Cooling profile	Main results
Andreini and Foster [79]	1974	Kinetics of solute removal during electron-beam and vacuum-arc remelting	Fe-Cu	Presented model for different melt rates	Presented model for kinetics of solute removal during electron-beam and vacuum-arc re-melting, which incorporates segregation behavior. Segregation coefficient for Fe-Cu, k=0.65.
Yuan, Sassa, Iwai, Wang, He, Asai [89]	2008	Copper distribution in Fe-Cu and Fe-C-Cu alloys under imposition of intense magnetic field	Fe with 0.4% Cu and Fe-3.95C-0.4 Cu	Held above liquidus 10-15 min, cooled to below the solidus over 60 min then quenched	Applying a 10T magnetic field makes a uniform micro distribution of Cu in the Fe-C-Cu alloy, but not the Fe-Cu alloy.
Sun, Guo, Vleugels, Van der Biest, Blanpain [90]	2012	Strong magnetic field processing of metallic materials: a review			Review of the principles and progress behind materials processing using strong magnetic fields.
Nakamota, Okumura, Tanaka, Yamamoto [91]	2014	Segregation of Cu by unidirectional solidification in molten Fe-C-Cu alloy	C-saturated iron with 0.5-3.7mass%Cu	Cooling rates 600 K/hr to 20 K/hr	Segregation coefficient, k=1.2. Starting with 0.3%Cu, could be reduced to 0.1%Cu by the end of the bar.
Xiao-Wei, Bai-Ling, De-Yang, Lin and En-Gang [92]	2016	Migration and alignment of Fe-rich particles in Cu under high magnetic field	Cu-30wt% Fe alloy		Applied a static 0.1 and 12 T and magnetic field and a field with a gradient of 92.1 T^2/m. Fe-rich particles can migrate upwards in the direction opposite gravity and tend to align along the direction of high magnetic field. The degree of alignment is related to external magnetic field strength, resistance force, effective time, initial condition of particles, etc.

Table S-14: Catalogue of studies for phase separation.

Authors	Year	Title	Main results
Yamaguchi, Ono, Usui [93]	2010	The equilibrium relation of immiscibility in an Fe-Cu-B system at 1873K	Investigated the Fe-Cu-B system for potential application in steel recycling. Confirmed separation between Fe-rich and Cu-rich phases, but the minimum mass%Cu in the Fe-rich phase was 20.

Table S-15: Catalogue of studies for applying solvent extraction to the melt.

Reference			Experimental details as available					
Authors	Year	Title	Solvent	Melt composition	T (ºC)	Contacting phases	Displacing equilibrium	Main results
Harald [94]	1925	Process for the treatment of alloys containing copper and iron, US Patent 1,562,472.	Lead					Pioneering study.
Langenberg and Lindsay [95]	1954	Removal of copper from iron-copper-carbon alloys			1600			Evaporation of lead noted as a significant issue. L=1.2-2.3.
Schenck and Perbix [96]	1962	Removal of copper from pig iron with lead and sodium sulphide slag		Pig iron	1400 to 1600	Droplets through the melt		Found L as a function of temperature from 1400 to 1600ºC: $\log(L_{Cu}) = \frac{1415}{T} - 0.552$
Imai and Sano [97]	1988	Copper partition between Na_2S fluxes and carbon-saturated iron melts		C-saturated iron	1150	Immiscible layers		L=2.4
Yamaguchi and Takeda [98]	2003	Impurity removal from carbon saturated liquid iron using lead solvent		C-saturated iron	1150	Immiscible layers	Recommended repetition or counter flow	L=2.2. By adding the same amount of lead to iron scrap, 70% of copper can be eliminated.
Yamaguchi, Ono and Usui [99]	2010	Oxidation removal of Cu from carbon-saturated iron via Ag phase	Silver	C-saturated iron	1250	Immiscible layers	1 atm oxygen atmosphere over Ag phase to promote oxidation of Cu	L between Fe-$C_{sat.}$ and Ag=7.15. Showed the Cu content of Fe-$C_{sat.}$ can be reduced from 4 wt% to 0.3-0.6wt% by oxidative removal via an Ag phase.

Yamaguchi and Ono [100]	2012	Oxidative removal of Cu from carbon-saturated via Ag phase into B2O3 flux		C-saturated iron	1250	Immiscible layers	B_2O_3-Al_2O_3-Ag_2O fluxes to promote oxidation of Cu	Greatest L between flux and Ag was 17 at 0.6 atm O and mole fraction B_2O_3 =0.42. Also performed numerical calculations for diffusion of the reactants and products.
Yamaguchi, Ono and Takeuchi [101]	2015	Removal of Cu in carbon saturated iron by sulfurization via Ag phase		C-saturated iron	1200	Immiscible layers	Na_2S-Cu_2S-Ag_2S fluxes to promote sulfidization of Cu	Greatest distribution ratio between flux and Ag was 42 with mole fraction Na_2S =0.4. Ag layer can prevent sulfidization of melt.
Rose [102]	1981	The extraction of copper from steel by molten electrolysis	Thorium					Noted possibility, but also noted impracticality with high melting point (1750ºC) and its radioactivity.

Table S-16: Catalogue of studies for slagging.

Author	Year	Title	Slag system	T (ºC)	Main results	Information provided by
Langenberg and Lindsay [95]	1954	Removal of copper from iron-copper-carbon alloys	FeS-Na_2S			Jimbo and Freuhan
Schenck and Perbix [96]	1962	Removal of copper from pig iron with lead and sodium sulphide slag	FeS-Na_2S	1200 to 1500	Investigated the mechanism of the reaction and sulfur content of metal. L=7-8.	
Markar, Dunning and Caldwell [103]	1968	Laboratory studies on the use of sodium sulfate for removing copper from molten iron	FeS-Na_2SO_4	Up to 1550	Investigated the efficiency of Na_2SO_4 slags. Found used slags were almost as effective as fresh Na_2SO_4 slags. Lump additions were more effective than powder. L=1.2-7.9. High temperatures and long slag reaction times tended to induce Cu and S reversion from the slag. Na_2SO_4 treatments were effective up to 1550ºC with reaction times of less than seven minutes.	Rose
Markar and Dunning [104]	1969	Use of sodium sulfate for copper removal from molten iron	Li_2SO_4, Na_2SO_4, K_2SO_4 , $MgSO_4$	1354 to 1649	Studied the quantitative relationship between copper removal and slag treatment using sodium sulphate additions. Also investigated other types of sulphates, but found Na_2SO_4 to be most effective. Increased efficiency by using lance injection and upgraded the scale to 0.5, 1 and 4 ton ladles.	Rose
Safiah and Sale [105]	1972	Influence of carbon on the removal of copper from iron melts with sulfide slags	Na_2SO_4	1550	Investigated mechanism of Cu removal, sulfur pickup and Na vaporization. Cu removal was 1.5 to 1.4% when C=0.01%, and 1.5 to 0.8% for C-saturated. Concluded sulfide slags are not effective at removing Cu from melts with low C. C is needed for the reaction with the sulfate.	
Markar and Brown [106]	1974	Copper removal from molten ferrous scrap: a pilot plant study				
Topkaya and Lu [107]	1974	Metal-slag-gas reaction and processes	Na_2S		Found gas/slag and metal/slag reactions and diffusion of Na in the gas phase to be rate controlling. L=24.	
Rose [102]	1981	The extraction of copper from steel by molten electrolysis	Cryolite with Cu_2S		Demonstrated electrolysis could be used to modify a ferrous melt beneath a sulfide-bearing slag, but modifications are needed for better current efficiency.	

Van Hecke, Fontainas [108]	1984	Process for extracting non-ferrous metals from iron-bearing scraps	Oxide-based		Scraps are heated a slagging agent for iron separates the iron contained in scraps.
Liu and Jeffes [109]	1985	Effect of sodium sulfide on removal of copper and tin from molten iron	Na_2S-FeS and CaO additions	1200 to 1350	Concluded that 70 wt%Na_2S-30 wt%FeS was the best composition and the addition of CaO improved the transfer of Cu to the slag while impeding the transfer of S to the metal. Found mass transport to be an important controlling step.
Okazaki and Robertson [110]	1985	Removal of tramp elements: mathematical modeling	Na_2S-FeS	1250	Modelled copper removal assuming mass transfer in the boundary layer to be rate controlling. L=25.
Oden and Elger [111]	1987	Removal of copper from molten ferrous scrap: Results of laboratory investigations	Na_2S-FeS-K_2O		Partitioned Cu into alkali or alkaline earth silicate slags or oxide-moderated sulfides. Unsatisfactory Cu removal.
Imai and Sano [97]	1988	The copper partition between Na_2S-bearing fluxes and carbon-saturated iron melts	Na_2S-FeS, as well as Li_2S , BaS, K_2S and CaS-FeS		Found favorable order as Na_2S>Li_2S>BaS>K_2S>CaS. 13%Na_2S resulted in L=21.5.
Jimbo, Sulsky, Freuhan [24]	1988	Refining of copper from ferrous scrap	FeS-Na_2S and Na_2S-FeS-Cu_2S-Cu systems	1400	Na_2S-FeS-Cu_2S-Cu systems can contain up to 36 wt% Cu_2S. 30%Na_2S resulted in L=20. 0.2FeS-0.8Na_2S has maximum copper removal.
Liu and Jeffes [112]	1989	Decopperization of molten steel by various slags	Na_2S, FeS, CaS, CaO, MgS and MgO based slags	1600	20-30% of initial copper was removed in 5 min.
Wang, Nagasaka, Hino, Ban-Ya [113]	1991	Copper Distribution between Molten FeS-NaS0.5 Flux and Carbon Saturated Iron Melt.	FeS-Na_2S	1400	FeS flux, L=9. Na_2S=0.4, L=24. Addition of 0.8 Na_2S decreases melt S content to 0.04%.

Wang, Nagasaka, Hino, Ban-Ya [114]	1991	Copper Distribution between FeS-Alkaline or -Alkaline Earth Metal Sulfide Fluxes and Carbon Saturated Iron Melt	Li_2S, K_2S, Sr_2S and BaS-FeS	1400	Li_2S-FeS flux, L=30. K_2S-FeS flux, L=20. SrS-FeS flux, L=22. BaS-FeS flux, L=19. Sulfur content decreases with addition of other sulfides to FeS.
КАШИН, et al. [115]	1991		Na_2CO_3 soda		Achieved copper percentages lower than 0.03% from 0.23-0.38%. Soda reacts with sulfur in melt to produce Na2S, but the reaction was difficult to control.
Katayama, Sano, Sasabe [2]	1996	Fundamental studies on removing residual elements from steel scrap	Na_2S and Na_2SO_4		Showed that flux could be recycled by leaching with water. The Na_2S and Na_2SO_4 components could be separated from the water.
Shimpo, Fukaya, Ishikawa, Ogawa [116]	1997	Copper removal from carbon-saturated molten iron with Al_2S_3-FeS flux	Al_2S_3-FeS	1200	L=28. Proposed a counter-flow method with recycling of the flux.
Cohen and Blander [117]	1998	Removal of copper from carbon-saturated iron with aluminum sulfide/ferrous sulfide flux	Al_2S_3-FeS	1365	L=30.
Kostetsky, Troyansky, Samborsky [118]		Removal of copper from carbon-iron melts	Fused soda block, soda and sulfur powders, mixtures of soda, sulfur and carbon powders	1250	Found at most 24% reduction in Cu from 0.64% Cu, but did not achieve consistent results.
Cohen [119]	2005	Removal of copper from iron-based metal with aluminum sulfide/ferrous sulfide matte	FeS-Al_2S_3 and sulfide-modified oxide fluxes	1365 and 1650	Al_2S_3 fluxes, L=30 but sulfur pickup was high. A sulfide-moderated oxide flux resulted in less sulfur transfer and could operate at 0.1wt% C for L=6.8, but it was thought this could be further optimized.

Hui, Jianjun, Shangxing et al. [120]	2009	Copper removal from molten steel with FeS-Na_2S slag	FeS-Na_2S-	1580	Found improved copper removal with increasing carbon, due to the increase in copper's activity.
Uchida, Matsui, Kishimoto, Miki [121]	2015	Fundamental investigation on removal of copper from molten iron with FeS-Na_2CO_3 fluxes	Na_2CO_3-FeS	1234 to 1404	Highest L=13.9, but high sulfur of 0.34%. Difference in distribution with Na_2CO_3 and Na_2S as starting materials attributed to difference in optical basicities.
Sasabe, Harada, Yamashita [122]	1996	Removal of copper from carbon saturated molten iron by using $FeCl_2$	$FeCl_2$ injections	1450	Injected $FeCl_2$ into molten iron. Iron chloride was vaporized in liquid iron and reacted with copper. Cu reduced from 0.7% to 0.5%. Calculated 18.5 kg $FeCl_2$ to reduce 1t from 0.5% to 0.1% and presented a rate equation for copper removal.
Hu, Yan, Jiang et al. [123]	2013		$CaCl_2$	1600	Investigated the selective chlorination of copper for Cu_2O-FeO by $CaCl_2$. Thermodynamic calculations showed copper could be selectively chlorinated by $CaCl_2$ and removed from the system.
Hu, Yan, Jiang et al. [123]	2013	Removal of copper from molten steel using FeO-SiO_2-$CaCl_2$ flux	FeO-SiO_2-$CaCl_2$	1600	Based on previous studies. Copper is partly oxidized and transferred to the flux as Cu_2O, then chlorinated by $CaCl_2$. Copper chlorides, CuCl or Cu_3Cl_3, evaporate. Acidic SiO_2 thought to promote chlorination and evaporation. Cu reduced from 1.29 to 0.74%.

Table S-17: Catalogue of studies for inclusion formation.

Authors	Year	Title	Main results
Oden and Elger [111]	1987	Removal of copper from molten ferrous scrap: results of laboratory investigations	Injected mixed oxides (copper-containing complex oxides, alkali silicates and complex alkali and alkaline-earth silicates and aluminates) with the purpose of forming copper-containing complex oxide inclusions, but was unsuccessful.

Table S-18: Catalogue of studies for filtration.

Authors	Year	Title	Main results
Zigalo et al.	1991		
Xiang et al.	1997		
Savov, Volkova and Janke [20]	2000	Copper and tin in steel scrap recycling	The above publications were not found, but this review reports that an Al_2O_3-ZrO_2 ceramic filter removes copper at a rate of 30%, as found by Zigalo et al. and Xiang et al.

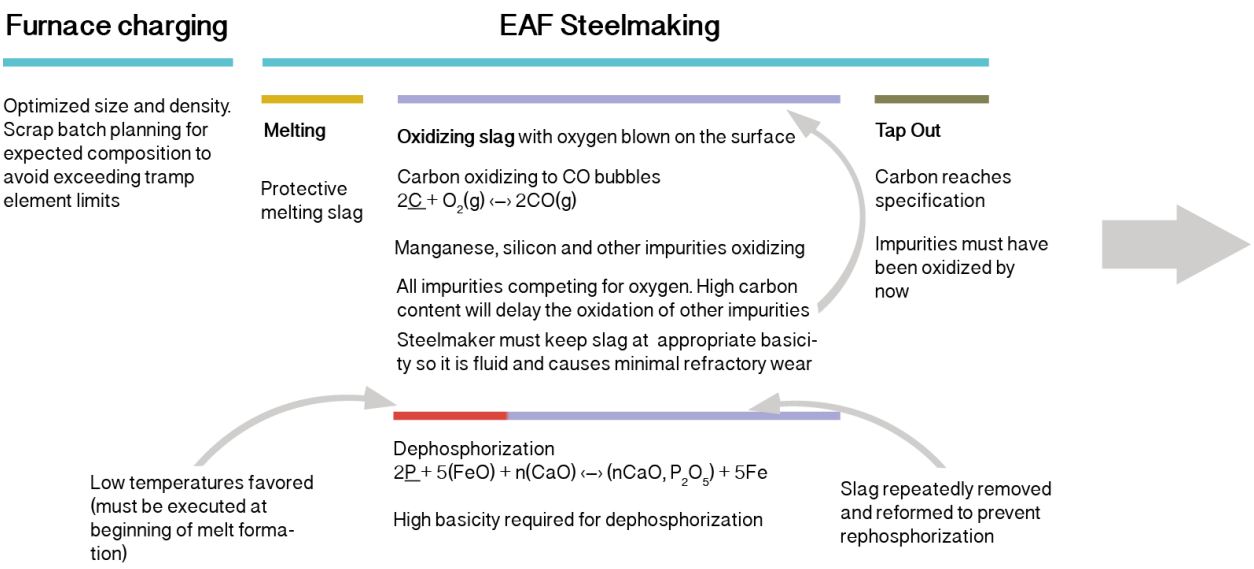

Figure S-3: Steps of EAF steelmaking.

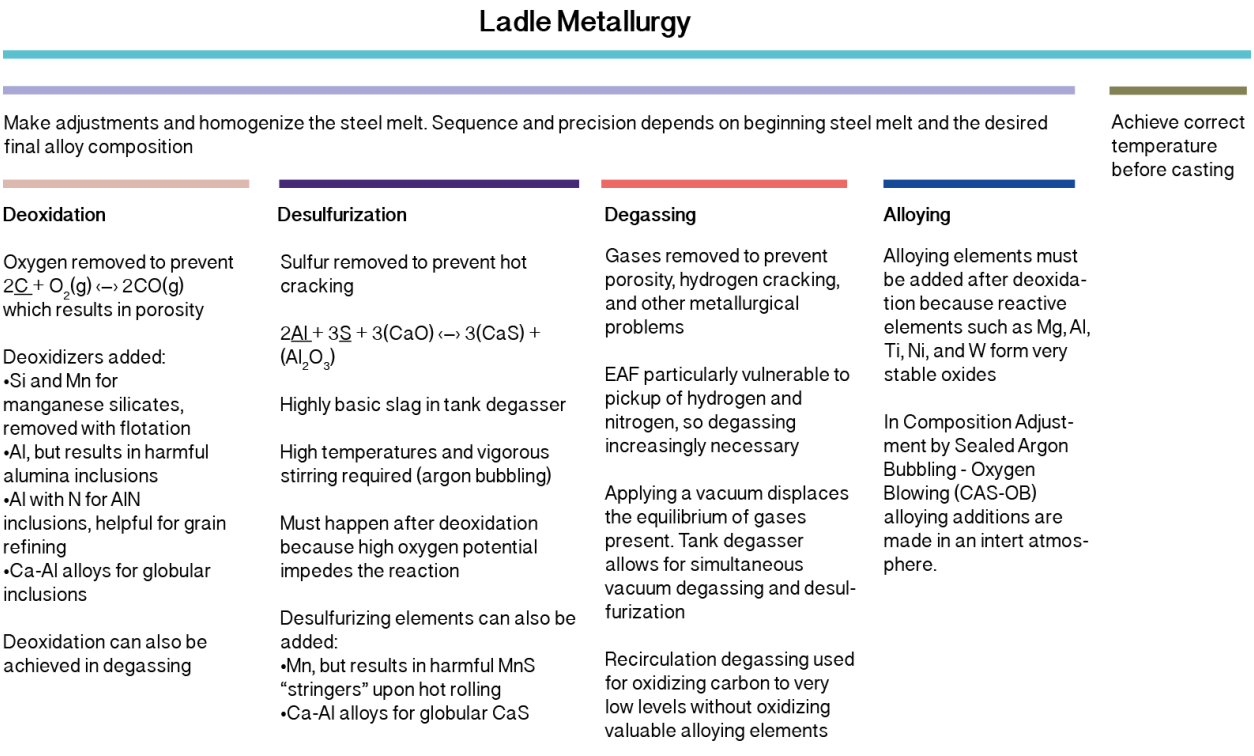

Figure S-4: Steps of ladle metallurgy.

Improved shredding and magnetic separation

Rate of copper reduction
Newell [3]: 0.1wt% Cu reduction with every 10-15lb/cubic ft (0.15 to 0.25 tonne/cubic m) higher-density shred from conventional shredded scrap (40-60 lb/cubic ft, 0.6-0.9 tonne/cubic m), which normally contains 0.4wt%Cu.

Scale-up reactor
A conventional hammer shredder could be used, operating at a lower process rate. Katayama et al. [2] show that repeating shredding and magnetic separation reduces copper content from 0.2 to about 0.14 wt%Cu. This could be repeated a third time to reduce to the range of 0.1wt% Cu. A dedicated high-density shredder could be developed as well to process scrap in one pass. Shredder outputs depend on horsepower, which could vary from 5 to 10,000. A typical shredding plant may process 100 t/hr, but rates vary from 25 to 250 t/hr [124]. Higher density comes with a slower process rate [1].

Energy consumption
Lassesson [125] reports that a modern Swedish shredding facility, which processes 70% iron, uses 15-20 kWh/ton input. Das et al. [126] report that 21 kWh/t is consumed in shredding vehicles. A more intensive shredding process with a slower rate, would use more energy. Here, we assume an additional pass through the shredder consumes an additional 20 kWh-t for 0.2wt%Cu, and a third pass would reduce copper content to 0.1wt% (but require a total additional 40kWh/t).

Material consumption
None directly.

Separate copper-rich fraction with sieve/trommel/ballistic separator

Rate of copper reduction
A range of copper concentrations are possible. Aboussouan et al. [4] report that 90% of copper initially present can be isolated by separating a certain size range of pieces from a conventional shredder. Newell [3] explains that their trommel system produces a scrap grade with 0.12-0.15wt%Cu. SICON [7] reports that a “clean” ferrous fraction can be obtained with their ballistic separator to divert copper meatballs. Shattuck and Ramsdell [9] report 0.16 to 0.17wt% Cu can be achieved with their ballistic system.

Scale-up reactor
Above, Aboussouan et al. [4], Newell [3], SICON [7] and Shattuck and Ramsdell [9] describe varying methods for separating scrap streams by size, magnetic permeability or density. Schulman [127] also describes sorting scrap streams by copper concentration using real-time bulk composition analysis. Industrial equipment is available, and could be operated by scrap processors or steelmakers.

Energy consumption
In general, trommels that separate scrap metal in a rotating cylindrical sieve or screen are highly energy efficient. Bianna Recycling [128] provide specifications for a range of trommels, which can process at most 210 m^3/hr with a power requirement of 30kW. Therefore, such a process should require on the order of 1kWh/t. More advanced technologies employing ballistics may not require significantly more energy. Shattuck and Ramsdell [9] report that their ballistic separator requires little electricity consumption and no air.

Material consumption
None directly.

Reactive gas applied to solid scrap

Rate of copper reduction
Tee and Fray [15] experimental results are used: copper reduction from 1wt% to below 0.05wt% in 10 minutes. The samples were 150 mg Fe, with copper winding, and the flow rate was 400/40 cm^3/min O_2/Cl_2 (at normal temperature and pressure) with the iron and copper sample at 800°C. An initial oxidizing treatment (O_2 blowing only) for 3 to 10 minutes at 800°C was recommended.

Scale-up reactor
Tee and Fray [15] describe a continuous dezincing plant by chlorination with a proposed capacity of 100,000 t/y. This process employs the same process conditions required for copper chlorination.

Energy consumption
Tee and Fray [15] estimate energy consumption of 27 kWh/tonne for the above chlorination plant, which assumes ferrous scrap initially at 800°C. An extra 10-20 kWh/tonne is added to account for heat losses during the transition from the process furnace to the EAF.

Material consumption

$$Cu(s) + Cl_2(g) \rightarrow CuCl_2(g)$$

To form $CuCl_2$ to eliminate 3kg of Cu/tonne steel, 3.3 kg $Cl_2(g)$ is required.

Embodied energy of Cl_2: 3.1 kWh/kg [129]

Embodied energy of Cl_2 consumed: 10.3 kWh/tonne steel.

For the amount of oxygen and iron consumed by oxidation, Tee and Fray [15] report an iron weight gain of approximately 0.01 g/cm^2, and that primarily Fe_2O_3 is formed. Assuming shredding produces scrap pieces about the size of a fist, the average shredded scrap piece was estimated as a sphere with a 5cm diameter, weighing 0.5 kg. With this average surface area, approximately 3 to 5 kg Fe/tonne steel would be lost, with 2 kg O_2/tonne steel consumed.

Embodied energy of O_2: 0.5 kWh/kg [130]

Embodied energy of O_2 consumed: 1 kWh/tonne steel.

Embodied energy of low-carbon steel: 7-8 kWh/kg [131]

Embodied energy of low-carbon steel consumed: 21-40 kWh/tonne steel.

The quantity of gas directly consumed is calculated, but a gas flow of 400/40 cm^3/min $O_2/Cl_2(g)$ was required in experiments, and a high gas flow would be required in the process.

Preferential melting

Rate of copper reduction

Brown and Block [16] experimental results were used, which showed negligible reduction in copper concentration due to adherence of liquid copper to the solid steel substrate, even as atmosphere varied from reducing, to inert and oxidizing conditions (unless liquation was achieved with a high initial copper concentration, >20wt%). Sano et al. [2] reported that the work of adhesion of liquid copper was minimized on magnetite and hematite, and this route could be theoretically feasible. Work has not been done to demonstrate a significant reduction in copper from typical scrap at low concentrations. Leak and Fine [18] demonstrate that an inert molten sweating medium and pre-coatings could prevent intimate

contact between liquid copper and the steel substrate, but their experiments used samples with high initial concentrations of copper to achieve liquation.

Scale up reactor
Scrap heating with rotation, vibration or shaking applied at temperatures above 1083°C. A continuous scrap heating system in a tunnel furnace, such as the one demonstrated by CONSTEEL [132], could be developed.

Energy consumption
Alternative heating designs are shown to be at least as efficient as conventional heating in the EAF. This treatment requires 10 additional minutes above 1083°C to collect liquefied copper. It is assumed that a tunnel furnace with a scrap conveyor is used. A conventional design is 2x2x20m [132], to contain 220 tonnes of steel scrap. Karimi and Saidi [133] report an overall heat transfer coefficient of 4 W/m^2K from the furnace walls of a pusher type reheating furnace for steel billets. Chen et al. [134] provide a break-down of the sources of heat output of a reheating furnace for steel billets. Roughly 18% of heat is lost from furnace walls, while 32% is lost as hot flue gas. Therefore, for a ten-minutes at 1100°C, it is calculated that 120 kWh is lost from the furnace walls, and 240 kWh is lost as hot flue gas. To overcome this loss at 40-60% efficiency, an energy input of 3 to 5 kWh/tonne steel is calculated. This treatment could be made continuous into the EAF, but an additional 10-20 kWh/t is accounted for the transition from the process furnace to the EAF.

Shaking: The documentation on rotary electric vibrators by [135] reports that the three phase 900 RPM model RE 185-8 max force 40,700 lbs. draws 43 A at 230 V = 10 kW. If 2 of these motors are used, 20 kW. For 10 minutes, less than 0.5 kWh/tonne steel is required.

Material consumption
No direct inputs.

Solvent extraction applied to solid scrap

Rate of copper reduction
Iwase [22] experimental results are used: reduction from 0.5wt% to 0.1wt% copper at 950°C with an Al-60 wt% Cu bath, followed by a second dip in a pure Al bath and mechanical vibration in between.

Scale up reactor
Two 90-tonne baths with liquid Al at 950°C, with a heated vibratory conveyor in between.

Energy consumption
Assuming the process is integrated into scrap heating and melting, such that scrap would be entering treatment at 950°C, sources of energy consumption are to heat Al added to the bath for each treatment, to maintain the Al baths at 950°C, to power the vibratory conveyor and compensate heat losses while scrap is transitioned from the process to the EAF.

Around 20 kg Al/tonne steel treated is lost for each treatment (see below). To heat the 20kg of Al added to the bath each treatment from 25 to 950°C, 7 to 10 kWh would be required (assuming 50-70% melt heating efficiency).

The Al baths are assumed to be 90-tonne channel furnaces for holding molten metal, as described by Schmitz and Trauzeddel [136]. For immersion, a liquid/solid ratio of 5 ml/g is assumed. With this ratio, approximately 7 tonnes of steel scrap could be treated in the 90-tonne Al bath. These furnaces consume 4 kW/tonne liquid metal to maintain temperature, so this totals 15 to 20 kWh/tonne steel for two ten-minute bath immersions. However, heat is lost when the furnace lid opens when steel scrap enters and leaves the bath. Schmitz and Trauzeddel [136] report 10kWh/tonne liquid metal is lost for having the lid open for 20 minutes, so 5 to 10 kWh/tonne steel is added.

The heated vibratory conveyor between Al baths is assumed to require 4 to 6 kWh/tonne steel (similar to heat and vibration requirements of preferential melting).

Total energy consumption is 42 to 60 kWh/tonne steel.

Material consumption
For scrap immersion, a liquid/solid ratio of 5 ml/g is assumed, which is a ratio of about 12 tonnes of Al/tonne steel scrap. The Al-Cu alloy generated from treatment is a valuable product, and thus is not considered as material consumption. However, the amount of Al adhering, and lost to oxidation in steelmaking, is considered as material consumption. Iwase [22] did not quantify the amount of Al adhering. Assuming shredding produces scrap pieces about the size of a fist, an average shredded scrap piece was estimated as a sphere with a 2.5cm radius, weighing 0.5 kg. If 0.5mm of Al adhered to the surface of each scrap piece, this would correlate to a loss of 20 kg Al/tonne steel treated.

Embodied energy of Al (primary): 56 kWh/kg [131].

Embodied energy of Al consumed: 1120 kWh/tonne steel.

Al oxidation in the EAF at 1600°C:

$$2Al + \frac{3}{2}O_2(g) = (Al_2O_3), \Delta H = -31000 \frac{kJ}{kg\ Al}$$ [137]

Heat generated: 172 kWh/tonne steel.

Matte extraction applied to solid scrap

Rate of copper reduction
Cramb and Fruehan [19] experimental results for 100 kg scrap were used, proving that copper concentration could be reduced from 0.4 to 0.1wt% Cu in a rotary kiln at 1-6 RPM after about 15 minutes.

Scale-up reactor
Rotary furnace, such as the continuous melting furnace described by Zhang, et al. [138].

Energy consumption
Assuming the scrap heating is at least as efficient as the conventional route, the initial temperature of the scrap is assumed to be 1000°C. The sources of energy consumption would be to heat the matte to 1000°C (heat content of industrial slag at 1000°C is 1 MJ/kg from Matousek [139], assuming heating efficiency of 40-60%, for 10kg matte/t steel, this equates to 5 to 6 kWh/tonne steel), maintain the scrap and matte at 1000°C for the 15 minute treatment (4 to 6 kWh/tonne, similar to preferential melting furnace requirements), rotate the scrap (1-2 kWh/tonne. The documentation on tilting rotary furnaces from Melting Solutions [140] shows a power requirement of 125 kW for motors to rotate 1 to 6RPM for 25t of scrap) and overcome any heat losses from the transition of scrap from the furnace to the EAF (10 kWh/tonne). Altogether, 20 to 26 kWh/tonne.

Material consumption
With an effective distribution ratio of 500, 10 kg of 82wt%FeS – 18wt%Na2S matte would be required for a reduction from 0.4 to 0.1wt% Cu.

Embodied energy of matte (general slag): 0.38 kWh/kg [141].

Embodied energy of matte consumed: 3.8 kWh/tonne steel.

Sulfur contamination of the scrap is noted, so a desulfurization treatment of the melt is required. Ghosh [142] provides a detailed report of desulfurization practice in secondary steelmaking. It is common to apply 10-25 kg slag/tonne steel. Sarna [143] reports a

temperature loss of 30°C can be expected. With powder injection and stirring, the total energy consumption is estimated as 20-30 kWh/tonne. Alternatively, Cramb and Fruehan [19] state that an acid wash following the matte extraction could prevent sulfur contamination, but this would not allow heat retention in the EAF route.

Embrittlement

Rate of copper reduction
Cho et al. [144] describe a system for removing copper from ferrous scrap by oxidation, mechanical impact and fluxing with an EAF slag while the ferrous scrap remains solid. There are various embodiments to the idea, described in the patent, but the above steps are reported to remove 99.5 to 99.9wt% copper in scrap initially containing 3 to 5 wt% copper. Therefore, it is assumed the final copper concentration is below 0.1wt%.

Scale-up reactor
The process requires a furnace for oxidizing scrap for 4 to 6 hours at 400 to 700°C. Thermal cycling or impact, such as vibrating or shaking, is required to aid in copper oxide spallation. Afterwards, the solid scrap is fluxed with an EAF slag at 1000 to 1200°C. For this step, a rotary furnace, such as the one described by Zhang et al. [138] is assumed.

Energy consumption
For the oxidizing step, a 2x2x20m tunnel furnace for 220t scrap with an overall heat transfer coefficient of 4 W/m^2K from the furnace walls is assumed (similar to the tunnel furnace assumed in preferential melting). For a 4 hour treatment at 500°C, heat losses from the furnace walls amount to 1280 kWh, with 2560 kWh for losses from hot flue gases (assuming similar heat output proportions to those reported by Chen et al. [134]). With an efficiency of 40-60%, this results in heat requirements of 30 to 45 kWh/tonne steel.

It is assumed that scrap would be shook by a conveyor in the tunnel furnace periodically throughout the oxidation treatment. Assuming that in total the scrap is shook for one hour, this amounts to 1 to 2 kWh/t.

For the fluxing treatment, a 15 minute treatment in a rotary kiln at 1000°C with 10 kg slag/tonne steel is assumed. This step is thus identical to the matte extraction process, so 20-25 kWh/t is attributed to this step.

Material consumption
Both CuO(s) and Cu_2O(s) form in the oxidizing step.

$$2Cu(s) + \frac{1}{2}O_2(g) \rightarrow Cu_2O(s)$$

$$Cu(s) + \frac{1}{2}O_2(g) \rightarrow CuO(s)$$

For 3kg Cu/tonne steel, this requires between 0.8 kg O_2(g) (assuming only Cu_2O forms) and 1.5 kg O_2(g) (assuming only CuO forms).

Embodied energy of O_2 consumed: 0.4 to 0.75 kWh/tonne steel [130].

For the fluxing step, it is assumed 10 kg slag/tonne steel would be consumed: 3.8 kWh/t [141].

Cho et al. [144] report that around 1% of iron would be lost to oxidation, e.g. 10 kg/tonne steel.

Embodied energy of O_2 consumed: 2 kWh/tonne steel.

Embodied energy of low-carbon steel: 7-8 kWh/kg [131].

Embodied energy of low-carbon steel consumed: 70-80 kWh/tonne steel.

Leaching

Rate of copper reduction

With ammonium carbonate solution

Oden, Adams and Fugate [29] explain that to dissolve metallic copper in ammonium carbonate solution, ammonium carbonate and metallic copper react to oxidize copper and form cuprous ammonium carbonate:

$$Cu^o + Cu(NH_3)_4^{2+} \rightarrow 2Cu(NH_3)_2^+$$

$$2Cu(NH_3)_2^+ + (NH_4)_2CO_3 + 2NH_4OH + \frac{1}{2}O_2 \rightarrow 2Cu(NH_3)_4^{2+} + 3H_2O + CO_2$$

The first equation does not proceed unless excess ammonia is present. Cupric ammonium complex is the active species. Re-oxidation of the cuprous species is a critical step, so oxygen must be supplied by vigorous aeration.

A well-aerated solution containing 10 to 30 g/l Cu, 68 g/l NH_3 and 44 g/l CO_2 achieved dissolution rates of 0.00156 g/cm^2/min. This rate is equivalent to 0.1-inch penetration per 24 hour period, sufficient to dissolve in 24 hours the thickest copper pieces observed in scrap. The treatment was followed by an ammoniacal rinse solution (1 hour with air agitation) and a water rinse. The solution was analyzed daily to maintain the necessary water, ammonia and CO_2. The ammoniacal rinse solution was regenerated daily by electrodepositing the copper. 0.3wt% was removed by the total treatment. Insufficient circulation of the leaching solution or incomplete removal of the leach solution during rinsing account for incomplete removal.

With ammonium chloride solution

Konishi et al. [36] explain that $Cu(NH_3)_4^{2+}$ can oxidize metallic copper, which is present in $CuCl_2$-NH_3-NH_4Cl solution. Konishi et al. [36] compared the leaching speed of copper in various concentrations of NH_3 and NH_4Cl and found leaching speed increased increasing NH_3 and NH_4Cl concentration, and proposed 4 kmol/m^3 NH_3 and 1 kmol/m^3 NH_4Cl and 0.5 kmol/m^3 Cu(II) as an optimum concentration. Leaching speed increased with stirring speed, described by the following equation.

$$R = k[Cu(NH_3)_4{}^{2+}]^{\frac{1}{2}} V^{\frac{2}{3}}$$

Industrially, stirring speeds of 200 RPM can be achieved, so the leaching speed of 2kg/m^{2}hr at 80^{o}C is used here. The authors found the leaching rate in chloride-based solutions to be superior to sulfate-based.

With ammonium sulfate solution

Konishi et al. [36] compared ammonium chloride and sulfate solutions, and found the chloride solutions to have a higher leaching speed. However, Sun et al. (2015) demonstrated that copper can be electrodeposited from an ammonium sulfate solution containing 51 g/l at a current efficiency of 89%. Sun et al. [145] did not report the leaching rate of the sulfate solution used, so the results by Konishi et al. are used. For a solution with 7 kmol/m^3 NH_3, 1 kmol/m^3 $(NH_4)_2SO_4$, 0.5 kmol/m^3 Cu(II) a leaching speed of 0.8 kg/m^{2}hr at 80^{o}C and 200 RPM was reported.

Scale-up reactor

Oden, Adams and Fugate [29] performed experiments on 100 kg scrap and recommended a tumbling reactor for scale-up. Jung and Keller [146] describe the dimensions and operating costs for hydrometallurgical processing of metals in gassed continuously stirred tank reactors on the order of 1000 m^3.

With electrowinning
Sun et al. [145] describe an electrochemical cell that can electrodeposit copper leached into solution (concentration greater than 50 g/l) with 90% current efficiency. This was demonstrated at a laboratory scale, so scale-up design is needed.

Energy consumption
With ammonium carbonate solution
The ammonium carbonate solution requires aeration and stirring. Jung and Keller [146] report that the power requirements of gassed continuously stirred tank reactors are driven by the agitator and compressor motor. Primary bioleaching reactors and vessels of 1000 m^3 typically require 250 to 315 kW for agitation and up to 300 to 500 kW for the compressor motor.

Assuming a ratio of 5ml leachant/g scrap in a 1000 m^3 tank, 180 tonne steel could be treated with 0.9 ML leachant. With the given leaching rate, 24 hours would be needed. Given the above power consumption, this would amount to 30-40 kWh/tonne for agitation and 40-65 kWh/tonne for aeration.

With ammonium carbonate solution
The ammonium chloride solution requires stirring and a higher temperature (80°C) to achieve the reported leaching rate. To raise the scrap to 80°C, 15-25 kWh/t is required. It is assumed that the process runs continuously, so the energy to heat the leachant to 80°C is not included. To calculate the energy to maintain the reactor at 80°C during the treatment, the heat loss is estimated. Documentation from Spirax Sacro [147] reports heat transfer coefficients from a steel surface to the atmosphere. A value of 12 W/m^2°C is used for a surface of 725m^2 (sides and top of a 10m diameter, 13 m high vessel treating 180 tonnes steel), amounting to 6,300 kWh for the treatment. With a heating efficiency of 40-60%, this accounts for 70-120 kWh/tonne steel. However, with 25 mm of insulation, this value would be reduced by 80%, to 15-25 kWh/tonne, and this case is used here. Stirring for 12 hours would require 15-20 kWh/tonne.

With ammonium sulfate solution and electrowinning
The ammonium sulfate solution has similar requirements to the ammonium carbonate solution above, but the treatment requires 24 hours.

For electrodeposition, Sun et al. [145] report that 2.1 kWh/kg Cu power is required with their set-up. With 3 kg Cu/tonne steel, this amounts to 6.3 kWh/tonne steel.

Prior incineration
The heat capacity of steel is 0.5 kJ/kg^{o}C. Assuming an efficiency of 40-60%, raising the temperature to 800^{o}C would require 185-280 kWh/t.

Material consumption
Assuming that dissolved copper is in the form of $Cu(NH_3)_4^{2+}$, 3.2 kg ammonia would be consumed per tonne of steel.

Embodied energy of ammonia: 7.9 kWh/kg [129]

Embodied energy of ammonia: 25.3 kWh/tonne steel.

The reactions above do not proceed unless excess ammonia is present. For the ammonium carbonate solution, there will be ammonia losses due to aeration. These losses are not accounted.

Distillation

Rate of copper reduction
Most studies on copper distillation have focused on understanding and optimizing the kinetics of the process. Harris [52] concluded that the 3 steps (transport from the melt to the reaction site, the reaction and transport away from the reaction site) fully describe the mechanism of vacuum distillation. These steps will be summarized here.

Liquid phase transport follows the same description used in the ladle treatment, so please refer to that section. For surface vaporization, the reaction at the interface and is described by the Hertz-Knudsen-Langmuir equation, which gives the rate of evaporation of solute atoms in a perfect vacuum. The rate constant, k^v, of this step is given below.

$$k^v = \frac{a_{Cu}\gamma_{Cu}^0 M_{Fe} P_{Cu}^0}{\rho(2\pi RTM_{Cu})^{\frac{1}{2}}}$$

The gaseous transport of copper atoms involves a combination of diffusion and convection, depending on the chamber pressure and surrounding gas flow. There are three main regimes:

1. Bulk flow of evaporating vapors is established with convection being the main transport mechanism. It is achieved when the melt vapor pressure is higher than chamber pressure or there is a flow of scavenging gas carrying away evaporating vapors. The rate constant, k^g, of

this step in this regime was determined by Harris as the equation below, with n_i being the flux of evaporating atoms in the gas phase (kg/m^{2}s), Z the total number of species in solution, and P_{ch} the chamber pressure (Pa).

$$k^g = \sum_{i=1}^{Z} n_i / P_{ch}$$

2. An intermediate regime exists when the chamber pressure is less than the total melt vapor pressure but more than that of the pure solvent. Here, both bulk flow convection and diffusion mechanisms are significant. Savov and Janke [66] found this regime to operate when the chamber pressure is 10-100 Pa and proposed the following empirical equation to determine k^g.

$$\log(k^g) = -0.45 \log(P) - 3.79$$

3. When the chamber pressure is greater than the melt vapor pressure there is significant resistance to transport and diffusion is the operating mechanism. Many studies have concluded refining in this regime to be entirely impractical.

Thus, since copper has a relatively low vapor pressure resistance in the gas phase is significant unless very low chamber pressures are achieved. When the total pressure is less than 10Pa, resistance is minimal, k_g approaches zero and atoms collide with cold walls to be removed by condensation. Ward found that experimental k_{Cu} values from levitated droplets are on average 65% of the theoretical maximum value predicted by the Hertz-Knudsen-Langmuir equation due to liquid-phase resistance. The overall rate constant, which is used in the first order rate equation, is determined by combining the rate constants of the steps above as shown below.

$$k_{Cu} = \left(\frac{1}{k^l} + \frac{1}{k^v} + \frac{1}{k^g}\right)^{-1}$$

The overall rate constant is not constant with respect to time because the gas phase transport coefficient is a function of the total flux evaporating from the steel surface and the total pressure of the vacuum chamber, which changes throughout the reaction. Harris recommends using a numerical solution, but most researchers measure and report the overall k_{Cu} value. The figure below compiles these results, with the corresponding source of the data shown in the table.

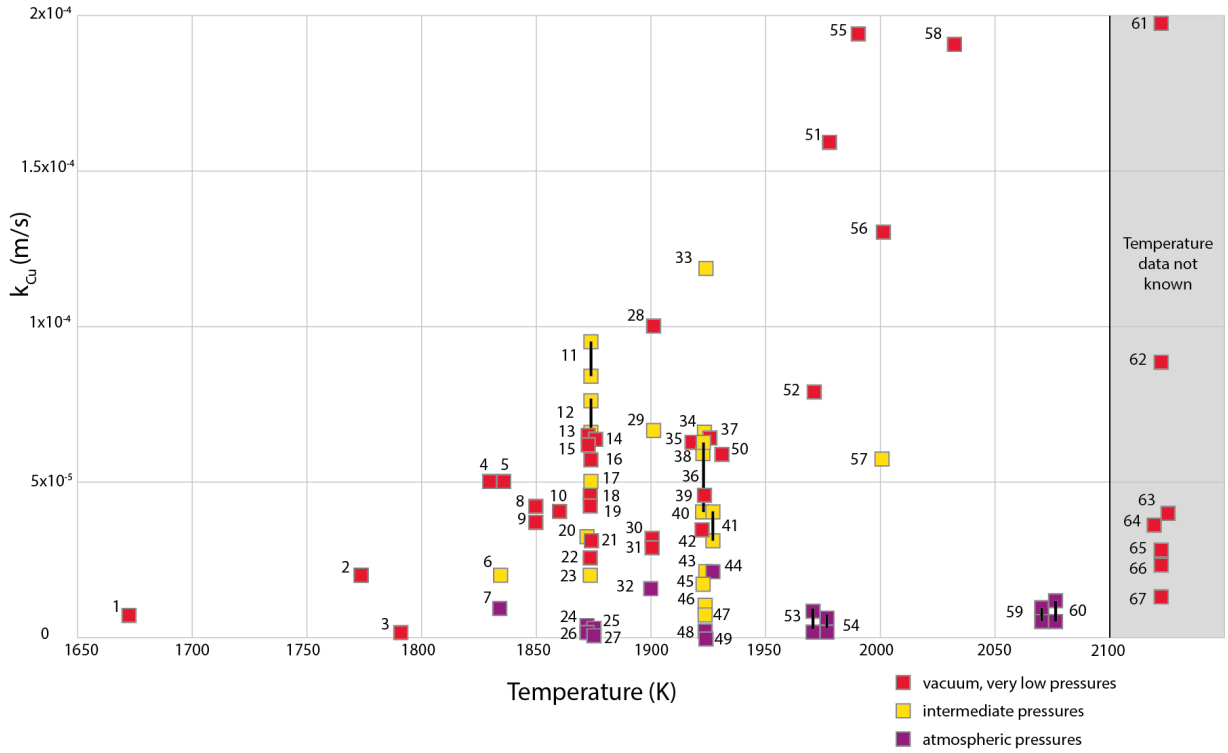

Figure S-5: k_{Cu} values in the literature as a function of temperature and pressure regime.

Table S-19: Information related to the data points in Figure S-5: chamber pressure, melt additions and reference.

#	Pressure (Pa)	Additions	Reference	#	Pressure (Pa)	Additions	Reference
1	10		Savov and Janke	35	8		Harris
2	10		Savov and Janke	36	133	with C	Ono-Nakazato et al
3	9	Sn, Mn, S additions to A36 steel	Harris	37	0.2		Nakajima et al
4	2.00E-02		Tokumitsu and Hirata	38	133	Fe-1.5Si-3C	Taguchi et al
5	10		Tokumitsu and Hirata	39	0.1, 1		Blacha and Labaj
6	20		Tokumitsu and Hirata	40	50		Nakajima et al
7	100		Tokumitsu and Hirata	41	133	with Si	Ono-Nakazato et al
8	vacuum	with induction stirring	Yamamoto and Kato	42	10		Blacha and Labaj
9	vacuum	without stirring	Yamamoto and Kato	43	100		Nakajima et al
10	10		Savov and Janke	44	1000	with Si	Ono-Nakazato et al
11	100	with MgO powder	Zaitsev et al	45	50		Blacha and Labaj
12	100	with SiO2 powder	Zaitsev et al	46	200		Nakajima et al
13	1		Savov and Janke	47	100		Blacha and Labaj

#	Pressure (Pa)	Additions	Reference	#	Pressure (Pa)	Additions	Reference
14	10	with 4% C	Savov and Janke	48	2000		Nakajima et al
15	1		Zaitsev et al	49	1000		Blacha and Labaj
16	10		Savov and Janke	50	7		Harris
17	100	with argon blowing	Zaitsev et al	51	0.01		Smith and Ward
18	0.1, 10		Zaitsev et al	52	11		Harris
19	vacuum		Ohno and Ishida	53	10000	with Si	Morales and Sano
20	50		Savov and Janke	54	10000	with C	Morales and Sano
21	10	Fe-Cr-Ni alloy	Savov and Janke	55	0.01		Smith and Ward
22	10	Reduced stirring	Savov and Janke	56	12		Harris
23	100		Savov and Janke, Zaitsev et al	57	20		Harris
24	10000	4% C with 1L/min Ar-H_2 flow	Jung and Kang	58	0.01		Smith and Ward
25	1000		Zaitsev et al	59	10000	with Si	Morales and Sano
26	10000	with 1L/min Ar-H_2 flow	Jung and Kang	60	10000	with C	Morales and Sano
27	100000		Zaitsev et al	61	vacuum		Ollette
28	10		Fischer et al	62	vacuum		Fischer, Janke and Stahlschmidt
29	100		Fischer et al	63	vacuum		Ward
30	7		Harris	64	vacuum		Ohno and Reiichi
31	vacuum		Fischer et al	65	vacuum		Harris and Davenport
32	1000		Fischer et al	66	vacuum		Salomon De-Friedberg and Davenport
33	100	with Ar gas flow, 4g/s SiO_2 and 340 kW plasma flame	Nishi et al	67	vacuum		Gill, Inveson, Wesley-Austin
34	130	with SiO_2 powder	Matsuo, Maya et al				

The highest values of k_{Cu} are achieved at very high temperatures and very low pressures. Increased temperature increases the vapor pressure of copper, which is 105 Pa at 1600°C, but increases to 430 Pa at 1730°C. These conditions are difficult to maintain at industrial scales, so significant work has been done to study k_{Cu} at intermediate pressures, around 100 Pa, to find favorable treatment times in a less demanding operating space. Parameters that could be varied to enhance the reaction in this regime include:

- Gaseous atmosphere type: The chamber is flushed with an inert gas, typically argon. Blacha et al. [73] explain that the type of gaseous atmosphere does have an effect on the diffusivity of evaporating vapors, but when the pressure is reduced below 1000 Pa, the impact drops significantly and ultimately fades out.

- Use of a scavenging gas: a scavenging gas can be used to dilute the vapors at the liquid/gas interface and establish a bulk flow of evaporating gases to a condensing surface.

- Additions to the melt: Blacha et al. [73] explain that evaporation rate depends on phenomena occurring on the interface and the key factors are the presence of a group of surfactants: oxygen, sulphur, selenium and tellurium. It is possible that a surface-active bath component causes the evaporation rate to increase. Carbon increases the activity of copper, with Jung noting that the evaporation rate increased about 2 times when liquid Fe was saturated by carbon, but within the normal carbon concentration range, 0.05 to 0.58wt%, Zaitsev et al. [70] noted that there was no perceptible effect on evaporation rate. Jung [77] investigated the evaporation rate of copper in the presence of sulfur, but found the highest rate to be achieved with an initial sulfur concentration of zero.

$$P_i = \gamma_i x_i P_i^0$$

Savov and Janke [66] concluded in order to apply vacuum distillation on a large scale, it will be necessary to optimize the thermodynamic conditions. They gathered thermodynamic data on activities of Cu and Sn in ternary and more complex iron-based melts and calculated the activity of Cu in the Fe-Si-Cu system. The most favorable conditions were realized at 15% Si in the melt. They suggested a process of recycling contaminated scrap in ferrosilicon production, but the results are not immediately relevant for typical low-carbon steel production.

The parameters above can increase k_{Cu}, but the specific surface area (A/V) is equally important in determining the refining time. A/V is determined by the reactor type, of which there are three main categories:

1. The liquid/gas interface exists only at the top surface, such as in a vat, but dimensions could range to a thin film.
2. Dispersing a gas through the melt.
3. Spraying the melt through the gaseous atmosphere/vacuum.

Therefore, in this analysis these three types of set-up's are defined as potential processes: vat with some recirculation (standard vacuum degassing), vat with bubbling and spraying

Scale-up reactor

Standard vacuum degassing

Adolf and Socha [137] describe the types of vacuum degassing: in the ladle, degassing in a stream and by lifting (Dortmund- Hüttenunion, DH and Ruhrstal-Heraeus, RH). The vat and lifting processes typically require 15 to 20 minutes. There are a range of chamber pressures typically achieved. 100 Pa is reported as typical, but 50 Pa or lower is possible. Because of this range, we define a minimal and a vigorous vacuum degassing process which should span the range of degassing processes currently in operation.

Minimal

The melt is stirred in the 160 tonne ladle described by Zaitsev et al. [70] (3.2m inner diameter, 2.9m height). Morales et al. [148] state that stirring increases the nominal surface area by a factor of 1.5 so the specific surface area, A, is set to 0.5m^{-1}. The chamber pressure is 100Pa and the total time is 10 minutes. Corresponding to 100Pa and 1600°C, k=2x10^{-5} m/s [66]. The final copper concentration was calculated to be 0.39wt%.

Vigorous

The melt is stirred re-circulated in a lifting process. Ostrava state that typically the melt is circulated three to five times. Therefore, we estimate the effective specific surface area as 2m^{-1}. The pressure of the vacuum chamber is reduced to 50 Pa (k=3x10^{-5} m/s, [66]). The process time is 30 minutes. The final copper concentration was calculated to be 0.35wt%.

Extended vacuum distillation with bubbling

The model proposed by Zaitsev et al. [70] is used, with the equation for the flux of copper under a vacuum accounting for argon blowing shown below.

$$J = \frac{p^0(Cu)\gamma(Cu)x(Cu)U\left(1+\left(\frac{\rho g H}{p_{atm.}}\right)\right)}{RT} + \frac{p^0(Cu)\gamma(Cu)x(Cu)}{\sqrt{2\pi RTM(Cu)}} k_{turb.}\left(\frac{\pi D^2}{4}\right)$$

Here, we set the chamber pressure, $p_{atm.}$, as 50 Pa. Zaitsev et al. [70] set $k_{turb.}$=3 for 100 Pa chamber pressure. Here, $k_{turb.}$ was set to 4 to correspond with the reduced pressure. U=0.14 m^3/s (gas-stream velocity), H=2.9m (height of metal column), D=3.2m (ladle internal diameter), $\gamma(Cu)$=10, T=1600°C (R is the universal gas constant and x(Cu) is molar concentration). The time to reduce to 0.1wt% Cu was calculated to be 130 minutes.

Bubbles could also be generated by a decarburization reaction. Nishi et al. [63] proposed applying SiO_2 powder to react with carbon in the melt and create CO(g) bubbles to increase the interfacial area. It was noted that this reaction is endothermic, so plasma heating was also applied to the surface to supply the heat needed for copper's vaporization. With this approach, k_{Cu} values similar to those attained at very low pressures could be attained at 130 Pa. Zaitsev et al. [70] also calculated that decarburizing the melt accelerates the process of copper extraction, as compared to evaporation from undisturbed surface, by a factor of 2.2-2.6 with SiO_2 and 2.8-3.1 times when MgO was used. However, because of the high carbon content required for the melt and simultaneous heating needed to overcome the endothermic reaction, this method of bubbling is difficult to incorporate into the conventional route and is not further considered in this analysis.

Extended spray distillation in vacuum

Winkler and Bakish [149] describe stream degassing for a 120 ton plant: typical treatment time is about 0.5s, but depends on the initial flow rate and height of the drop. Upon release into the vacuum, the melt disperses into drop sizes typically 1 to 5mm in radius.

Here, we set the vacuum pressure to the lowest possible reported by Winkler and Bakish [149] for ladles: 10 Pa. At this pressure, $k=6.5x10^{-5}$ m/s. With this low chamber pressure, a droplet diameter of 1mm is assumed for a specific surface area of $6{,}000m^{-1}$, so the time to reduce to 0.1wt% Cu was calculated to be 4s. The reactor would need to be adjusted to allow for this extended treatment time, either with a greatly increased falling distance, or multiple circulations of the melt.

Energy consumption

Standard vacuum degassing

The most significant source of energy consumption for vacuum treatments is overcoming the heat losses during treatment. Lange [150] provides the change in temperature for RH-type, DH-type and tank degassing processes, reporting that there is a temperature drop of at least 50°C. This requires 16-22 kWh/t of heat to overcome.

Ghosh [142] provides rates of temperature loss for different ladle (200t) treatments. For circulation degassing, the rate is 0.7-1.5 °C/min, and for ladle holding the rate is 0.5-1°C/min. Assuming it takes 10 minutes to reach the chamber pressure, about 5 kWh/t of heat would be needed for holding during this time. The temperature drop could be as low as 10°C during the minimal treatment, requiring 5 kWh/tonne steel. Ghosh [142] notes that temperature losses in prolonged treatments of the melt can be as high as 100°C. For the

more vigorous treatment, a temperature loss of 70°C is assumed, requiring 25-40 kWh/tonne steel of heat.

To generate a vacuum, Kustenov and Kats [151] show the energy consumption for mechanical pumps is about 1 kWh/ton liquid steel for a 90t vacuum degassing unit. An energy requirement of 1-2 kWh/tonne steel is assumed here.

Overall, it was estimated that standard vacuum degassing treatments require 15-50 kWh/tonne steel.

Extended vacuum distillation with bubbling
Ghosh [142] reports that the temperature loss for a 200t ladle during gas purging is 1-2°C/min. With this rate, the total temperature loss would be 130-260°C. Heat would need to be delivered during treatment: 70-140 kWh/tonne steel (roughly estimated from the constant heat loss rate).

With the extended treatment, the vacuum would need to be maintained and the argon flow rate increases the pumping requirement. However, Burgmann and Göhler [152] state that the mechanical pumping system is well-suited for compensating for constant volume flow rates. The energy requirement for argon blowing within the vacuum system is estimated as an additional 10-20 kWh/tonne steel.

Extended spray distillation in vacuum
The heat loss of a liquid metal stream is difficult to model as surrounding droplets can shield radiation losses. Michaelis et al. [153] describe this "caravan effect" – that each droplet experiences a unique cooling profile dependent on its position and the character of the stream. Most models are for the cooling of a single droplet. Here, we use the observed heat losses from a 120 ton plant during 0.5s stream degassing reported by Winkler and Bakish [149], below:

T loss due to heat absorbed in tap ladle: 24°C
T loss due to heat absorbed in vacuum ladle: 28°C
T loss due to heat absorbed in limiter, nozzle, etc: 3°C
T loss due to heat lost by radiation: 50°C

The heat lost by radiation is proportional to the effective time for radiation to take place and the area from which it is radiating, and the nature and temperature of the receiving surface. Heat loss is dependent on the geometry of the system, but radiation heat losses are expected to be proportional to time and the relative radiating and receiving areas.

Extending the treatment from 0.5s to 4s and decreasing the droplet size from 2-10mm to 1mm in diameter, results in (A*Δt) effectively increasing by a factor of 14. Applying this factor to the radiation heat loss, particles would certainly solidify, so heat must be supplied during treatment. Winkler and Bakish [149] noted that their system could be further optimized with the use of a heat shield. Here, we estimate that heat would need to be supplied to overcome an equivalent temperature drop of 400-500°C. With the assumed efficiency of 50-70%, this equates to 125-220 kWh/tonne steel.

Material consumption
None directly.

Reactive gas evaporation

Rate of copper reduction
Hidani et al. [82] provide the average rate constant of $3.3x10^{-5}$ m/s at 1600°C for intermediate pressures 100-100,000 Pa when NH_3 is blown on the melt at 2L/min. The authors note that boiling occurred, so the specific surface area increases. Tayeb et al. [154] note that intense reactions in the ladle can increase the specific surface area by 3 to 14 times the nominal value, but Ghosh [142] reports a factor of 100 for emulsification. A value of $10m^{-1}$ is used here.

Scale-up reactor
NH_3 is blown onto the melt under reduced chamber pressure, assumed to be 200Pa. With $k=3.3x10^{-5}$ m/s and $A=10m^{-1}$, the time to reduce to 0.1wt%Cu was calculated to be 60 min.

Energy consumption
The reactions occurring have not been confirmed, so the heat generated/absorbed is unknown. As the reaction generates a large surface area, heat loss would be greater from the exposed surface area. Ghosh [142] states that powder injection in a 200t ladle results in a temperature loss rate of 2-3.5°C/min. Assuming a similar heat loss rate, this process results in a temperature drop of 120-210°C, requiring 45-115 kWh/tonne steel heat to compensate.

Similar to argon blowing, the chamber pressure must be maintained with increased pumping requirements for blowing NH_3. 10-20 kWh/tonne is allocated.

The melt supersaturates with nitrogen. Hidani et al. [82] note that a 30 minute vacuum degassing treatment would be required afterwards. Above, it was determined that such a treatment requires ~50 kWh/tonne.

Material consumption
The reaction proposed by Hidani et al. [82] is:

$$\underline{Cu}(l) + \frac{1}{2}H_2(g) \rightarrow CuH(g)$$

Where hydrogen is provided by NH_3(g) dissociating into nitrogen and hydrogen gas:

$$NH_3(g) \rightarrow \frac{1}{2}N_2(g) + \frac{3}{2}H_2(g)$$

0.3 kg of NH_3 would be consumed per tonne of steel.

Embodied energy of ammonia: 7.9 kWh/kg [129]

Embodied energy of NH_3 consumed: 2.4 kWh/tonne steel.

Ladle melt treatment

Rate of copper reduction
In the absence of kinetic data, we assume this liquid-liquid process would be similar to other liquid-liquid steel refining reactions. Bodsworth [155] states that steelmaking interface reactions are transport-controlled within a few minutes of the start of the reaction, when a concentration gradient has been established.

The mass transfer of a solute between two liquid phases in interfacial equilibrium is given by the equation below.

$$\dot{m} = kA\left([x]_i^{phase\ 1} - \frac{[x]_i^{phase\ 2}}{L}\right)$$

The rate constant, k, is usually determined by transport in the melt, k_m [156]. The rate constant in slag, k_s, is usually of similar magnitude [148]. Therefore, here we estimate k_m. Several approaches exist.

- *Machlin's model:* If the liquid metal is being mixed, mass transfer of the solute element can be described by the model developed by Machlin [157] using surface renewal theory. The following equation gives the rate constant, k_m, of copper to the surface, where v is the surface velocity of the melt (m/s) and r is the radius of the crucible (m). Melt velocity is difficult to determine. Sheng and Irons [158] found this value to be 0.2 m/s in induction melting furnaces. The values for melt velocity with new induction stirring in ladle furnaces was found to be 0.5 to 1 m/s. Ovako steel reported a melt velocity of 0.7 m/s [159].

$$k_m = \left(\frac{8D_l v}{\pi r}\right)^{\frac{1}{2}}$$

- *Higbie's and Danckwerts model:* Higbie's surface renewal theory is applicable when the flow at the interface is laminar. In a slag-metal system, the slag would tend to flow like a rigid body. Mass transfer at the interface in the high viscosity phase would be exclusively by molecular diffusion. Since the surface gets renewed continuously it was derived that, where t_e is the time of exposure of the rigid body:

$$k_m = 2\left(\frac{D_l}{\pi t_e}\right)^{\frac{1}{2}}$$

  In turbulent flow, Danckwerts derived that:

$$k_m = (D_l S)^{\frac{1}{2}}$$

  S varies between 5 to 25 per second for mild turbulence, and up to 500 per second for violent turbulence [142].

- *k_mA/k_m and mixing power density:* In stirred systems it is difficult to measure the contact surface area, A so a total k_mA parameter is experimentally determined as gas flow rate, Q, or mixing power density, ε, is varied. There are many results available which relate rate constants for slag-metal reactions with stirring gas flow rate. The relationship below has been found to be generally useful, as provided by Lange [150], where k_p is in (1/min) and specific stirring power, ε (kW/t).

$$k_p = 0.14\varepsilon^{0.68}$$

  Electromagnetic stirring is reported to have a stirring intensity of 0.05 W/kg [160], while modern Argon practice has a stirring intensity of 0.006 W/kg [142].

Diffusivities

In the above models, the diffusivity value, D_l, of copper in the melt is important. The values in the table below are diffusion coefficients relevant to the copper-iron system found in the literature.

Table S-20: Diffusivities of copper in liquid iron found in the literature.

D_{Cu} (m^2/s)	Reference	Notes
$2x10^{-8}$	Davenport, Bradshaw and Richardson	Most liquid metals
10^{-8}	Harris	
$4.15x10^{-8}$	Ono and Ishiboti	carbon-saturated iron from 1623-1823K
$5x10^{-8}$	Iida and Guthrie	
$D_{Cu}=14.6x10^{-8}$ exp(-9700/RT)	Blacha and Labaj	Darken equation for binary solutions
$5x10^{-9}$	Lange	

Overall range

The values in the table below were calculated by the different models. The Iron and Steel Institute provided a range of values as well, saying the mass transfer coefficient of should is at least 10^{-4} m/s, and at most 10^{-2} m/s. Morales (2015) calculated k_m to be 1 to $53x10^{-4}$ m/s. Engh [160] showed k_m variations of 3 to $50x10^{-4}$ m/s.

Table S-21: Range of variables used to calculate k_m.

Variable	D_{Cu} (m^2/s)	Melt velocity (m/s)	S (1/s)	Stirring power density (W/kg)
min	$5x10^{-9}$	0.2	10	0.006
max	$4.15x10^{-8}$	1	100	0.05

Table S-22: Range of values calculated for k_m.

Calculated k_m from range of variables (m/s)	Machlin's model (furnace radius 1.5m)	Danckwert's model	k and stirring density	Individual mass transfer coefficient	Iron and Steel Institute range
Min	$4.12x10^{-5}$	$2.24x10^{-4}$	$1.83x10^{-4}$	$7.00x10^{-4}$	$1.00x10^{-4}$
Max	$2.65x10^{-4}$	$2.04x10^{-3}$	$4.32x10^{-3}$	$3.70x10^{-3}$	$1.00x10^{-2}$

Here, we assume the value of k_m to be $5x10^{-4}$ m/s.

For specific surface area, the interfacial area with stirring is typically 1.5 times [148] or 3 to 14 times [154] the nominal surface area. Here, we use a value of $1m^{-1}$, which is typical for ladles with intense stirring.

The values of L, distribution ratio, have been determined for copper between the melt and the various slag/solvent compositions. The distribution ratios for most of the compositions in Figure 3 (main text) are too low to use industrially. Here, we use the most optimized slag composition, FeS-Al_2S_3 with L=30 [117].

To reach 0.1wt%Cu in the melt, a treatment time of 50 minutes was calculated.

Scale-up reactor
This treatment would be an additional step in the ladle. The ladle would have similar dimensions to the 160 tonne ladle described by Zaitsev et al. [71] (3.2m inner diameter, 2.9m height). It would be stirred with argon (typical rates of 0.14 m^3/s), or electromagnetically.

Energy consumption
In order to increase the distribution of copper to the slag, the melt must be carburized (and subsequently decarburized), and at a low temperature, 1365°C. It is assumed that the melt is initially at 1600°C, and during carburization the temperature is decreased to 1365°C. The main sources of energy consumption would be heating the quantity of slag, maintaining treatment temperature, stirring and returning to 1600°C after treatment.

Heating 100 kg slag to 1365°C: heat content of industrial slag at 1000°C is 1 MJ/kg [139]. With heating efficiency of 50-70%, for 100kg slag/t steel, this equates to 40-50 kWh/tonne steel.

Heat loss during treatment: The main source of heat loss would be conduction through the ladle sides and bottom, as a thick slag layer often radiation from the top, such that radiation heat losses are negligible [150]. Alexis et al. [161] report the measured conduction heat loss rate from the sides and bottom of a 100 ton ladle furnace to be 12.5 kW/m^2. With the dimensions above, the ladle sides and bottom have a surface area of 40 m^2. Therefore, the heat loss during treatment is around 500 kWh, requiring 4-5 kWh/tonne steel.

Stirring: Thrum [162] compares induction and gas stirring in ladle furnaces. The power consumption of electromagnetic stirring is about 1kW/tonne steel, so roughly 1 kWh/t is required in this treatment.

Decarburization: The melt would be carburized before treatment. To continue in the EAF route, the melt would be decarburized following treatment. The melt must also be heated to 1600°C following the 1365°C treatment temperature. During decarburization, heat is supplied:

$$\underline{C} + \frac{1}{2}O_2(g) \rightarrow CO(g), 2.55\frac{kWh}{kg\ C}\ [163]$$

With 43 kg C/tonne steel, this generates 109 kWh/tonne. 75-100 kWh/tonne heat is required to raise the temperature of the melt from 1365 to 1600°C, so the heat generated by the decarburization reaction should be sufficient.

Material consumption

The treatment requires a significant quantity of slag. From the equilibrium distribution ratios in Figure 3 (main text), the following quantities were calculated per tonne steel:

Table S-23: Calculated quantities of solvents and slags needed to treat one tonne of steel from 0.4 to 0.1wt% for the reported equilibrium ratios.

Solvent/slag	kg/tonne
Lead solvent	1246
Silver solvent	419
0.6 FeS-0.4 Na_2S slag	125
0.8 FeS-0.2 K_2S slag	150
0.7 FeS-0.3 Sr_2S slag	136
0.2 FeS-0.8 Al_2S_3 slag	100
S-modified oxide slag	441
FeO-SiO_2-$CaCl_2$ slag	600

To calculate the embodied energy, the ICE Database [141] reports slag has an embodied energy of 0.44 kWh/kg. The above slags have different compositions and would have different embodied energies, but in the absence of this data this general figure is applied to all slags. For the lead and silver solvents, an embodied energy of 7.5 and 430 kWh/kg (primary) is reported [131].

The above distribution ratios were achieved with carbon-saturated melts. Carbon-saturation increases the activity of copper and the temperature of the melt can be reduced, such that the exothermic reaction of copper to copper sulfide progresses further. To saturate the melt, 43

kg C/tonne steel is required. Coal has an embodied energy of which has an embodied energy of 5.8 kWh/kg [164], assuming a similar value for metallurgical coal, this corresponds to 250 kWh/tonne steel.

In decarburization, assuming CO(g) is formed, 53 kg O_2(g) is required, with an embodied energy of 0.5 kWh/kg [130], which totals 27 kWh/tonne steel. This reaction produces 96 kg CO(g)/tonne steel.

The melt is contaminated with sulfur by the FeS-Al_2S_3 slag. A desulfurization treatment would be requires, which typically requires 10-25 kg slag and 20-30 kWh/tonne steel energy ([142] and [143]). However, the sulfur concentrations from the contamination are much higher than amounts typically encountered in steel refining, so a more intensive treatment may be required.

Unidirectional solidification

Rate of copper reduction
Nakamoto et al. [91] show that the partition coefficient, k, of copper in carbon-saturated iron is 1.2. The cooling rate that resulted in the greatest gradient was 60°C/hour in their experimental work. With the given partition coefficient, the gradient would decrease from 0.4wt% Cu to about 0.32wt% during solidification.

(Note that the catalogue shows some preliminary investigations which use a magnetic field during solidification to migrate copper within an Fe-C-Cu alloy. Applying a magnetic field is not included in this analysis as a scalable reactor does not exist in steelmaking).

Scale-up reactor
A slow cooling rate would be required during casting and solidification. The furnace could be similar to an in-line tunnel furnace used for keeping billets at high-temperature from casting to rolling.

Energy consumption
[129] show in-line tunnel furnaces consume about 200 kWh/tonne steel. These furnaces hold steel over 1000°C for several hours. This treatment requires 6.5 hours, so this requirement is multiplied by 2-3, for 400 to 600 kWh/tonne.

Material consumption
None directly.

Vacuum arc re-melting

Rate of copper reduction

Andreini and Foster [79] developed a model of the process to predict the degree of refining of solute elements and applied it to automotive scrap and compared it to experimental results.

The authors introduced a dimensionless constant, β. When β>1, the magnitude of β can indicate the extent to which refining will occur during the process. The equation below gives the formula for β, where k_i is the distribution coefficient of the species, α_i is the evaporation coefficient of the species, P_i^0 is the vapor pressure of the pure species and γ_i is the activity coefficient, and j denotes the melt species.

$$\beta_i = \frac{\alpha_i \gamma_i P_i^0}{\alpha_j \gamma_j P_j^0} \left[\frac{M_j}{M_i}\right]^{\frac{1}{2}} (k_i)^{-1}$$

Scale-up reactor

Scholz et al. [80] reviewed the technology and equipment available for vacuum arc re-melting. They report that tramp elements such as Pb, Sn, Bi, Te, As and Cu will be removed, and their level can be adjusted with the vacuum pressure.

Scholz et al. [80] provide the key operating parameters for VAR, given in the table below. The ingots may be up to 1300mm in diameter and 30t in weight.

Table S-24: Representative operating parameters in VAR.

Stock diameter (m)	0.9
Energy consumption during re-melting (kWh/t)	700
Melting rate (kg/min)	9

Applying these parameters to the model presented by Andreini and Foster [79] and an initial concentration of 0.4wt%, a treatment would lead to a final concentration in the range of 0.2wt%. The treatment could be repeated, or a slower melting rate or lower chamber pressure could be employed to further reduce the final copper concentration.

Energy consumption

Scholz et al. state that the power consumption of the process depends mainly on the alloy to be remelted, with the specific heat of the material to be the most important factor as it

determines the arc formation. Minor influences are the gas load of the material and the suction capacity of the pumping system and electrical efficiency.

Therefore, the energy consumption is close to the re-melting energy, 700kWh/t. Krüger et al. [165] report that the electroslag refining steel can consume up to 1300 kWh/tonne. For a more intensive process which reduces copper concentration to 0.1wt%, this higher end of energy consumption is assumed.

Material consumption
None directly.

Ceramic filtration

Rate of copper reduction
The original publications could not be found, but Savov and Janke [66] report that an Al_2O_3-ZrO_2 ceramic filter removes copper at a rate of 30%, as found by Zigalo et al. and Xiang et al.

Scale-up reactor
Ghosh discusses that ceramic filters have been used to remove inclusions from the melt for low-melting nonferrous metals such as aluminum. For steel melts, active research and development work is being pursued. Ghosh [142] reports that the mass flow of steel with a filter is slowed by 0.25 to 0.6.

Here, we assume a filter is incorporated into tapping such that the time for tapping doubles.

Energy consumption
Yin [166] reports a temperature drop of around 70°C during tapping. Assuming that the slower tapping due to filtration causes an additional 70°C temperature drop, this would require 20-30 kWh/tonne steel heat to recover.

Material consumption
None directly, but contamination of the melt by ceramic particles is possible.

References

[1] S. Newell: *Int. Conf. on Recycling in the Iron and Steel Industry*, 1996.

[2] N. Sano, H. Katayama, M. Sasabe, and S. Matsuoka: *Scand. J. Metall.*, 1998, vol. 27, pp. 24-30.

[3] S. Newell: *UK Electric Steelmakers*, presentation, May 2017.

[4] L. Aboussouan, P. Russo, M.N. Pons, D. Thomas, J.P. Birat, D. Leclerc: *Powder Technol.*, 1999, vol. 105, pp. 288-294.

[5] A.D. Shulman: *U.S. Patent No. 7,886,915*, 2011

[6] P. Russo: Jernkontoret scrap seminar in Hofors, Sweden, 2014.

[7] SICON: PrimeScrap (2018), https://sicontechnology.com/en/sicon-primescrap/. Accessed January 2019.

[8] STEINERT: SteelMaster (2018), https://steinertglobal.com/us/magnets-sensor-sorting-units/magnetic-separation/magnetic-head-pulleys/steinert-steelmaster/. Accessed January 2019.

[9] M. Shattuck and C. Ramsdell, The case for producing low-copper steel with ballistic separators (Waste Advantage, 2018) https://wasteadvantagemag.com/the-case-for-producing-low-copper-steel-with-ballistic-separators/. Accessed January 2019.

[10] A. D. Hartman, L. L. Oden and D. L. Davis: *Iron Steelmaker*, 1994, vol. 21, pp. 59–62.

[11]A. D. Hartman, C. A. Williamson and D. Davis: *Iron Steelmaker*, 1996, vol. 23, pp. 43–45.

[12] K. Matsumaru, M. Susa, and K. Nagata, K: *Tetsu-to-Hagane*, 1996, vol. 82, pp. 799-804.

[13] J.K.S. Tee, and D.J. Fray: *JOM*, 1999, vol. 51, pp. 24-27.

[14] J.K.S. Tee, and D. J. Fray: *Int. J. Miner. Process. Extr. Metall.*, 2004, vol. 113, pp. 129-138.

[15] J.K.S. Tee and D.J. Fray: *Ironmaking Steelmaking*, 2006, vol. 33, pp. 19-23.

[16] R.R. Brown, and F.E. Block: *U.S. Dept of the Interior, Bureau of Mines,* 1968.

[17] G.W. Elger: *U.S. Dept. of the Interior, Bureau of Mines*, 1968.

[18] V.G. Leak, M.M. Fine, and H. Dolezal, H.: *U.S. Dept of the Interior, Bureau of Mines,* 1973.

[19] A.W. Cramb, and R.J. Fruehan: *Iron Steelmaker*, 1991, vol. 18, pp. 61-68.

[20] L. Savov, E. Volkova, and D. Janke: *Materials Geoenviron.*, 2003, vol. 50, pp. 627-640.

[21] M. Iwase, and K. Tokinori: *Steel research*, 1991, vol. 62, pp. 235-239.

[22] M. Iwase, M., and H. Ohshita: *Steel Research*, 1996, vol. 65, pp. 362-367.

[23] M. Iwase: Iron and Steel Society, Warrendale, PA, 1996.

[24] I. Jimbo, M.S. Sulsky, and R.J. Fruehan: *Iron Steelmaker*, 1988, vol. 15, pp. 20-23.

[25] R.J. Leary: *Dept of the Interior, Bureau of Mines* 1965.

[26] C.J. Herter: U.S. Patent No. 4,517,016, 1985.

[27] W.D. Cho, P. Fan, G. Han, and K. Rhee: *AISTECH-Conference Proceedings,* 2004, vol. 1, p. 861.

[28] W.L. Staker, C.J. Chindgren, and K.C. Dean: U.*S. Dept. of the Interior, Bureau of Mines*, 1971.

[29] L.L. Oden, A. Adams, and A.D. Fugate: *U.S. Dept. of the Interior, Bureau of Mines,* 1972.

[30] D.T. Chin: *AIChE Journal*, 1977, vol. 23, pp. 434-440.

[31] H. Majima, S. Nigo, T. Hirato, Y. Awakura, and M. Iwai: *Shigen-to-Sozai*, 1993, vol. 109, pp. 191-194.

[32] K. Zhou, K. Shinme, and S. Anezaki: *J. MMIJ*, 1995, vol. 111, pp. 49-53.

[33] X. Meng, and K.N. Han: *Min. Proc. Extrac. Metall. Rev.*, 1996, vol. 16, pp. 23-61.

[34] K. Koyama, M. Tanaka, and J.C. Lee: *Mater. Trans.*, 2006, vol. 47, pp. 1788-1792.

[35] Y. Lim, O.H. Kwon, J. Lee, and K. Yoo: *Geosystem Engineering*, 2013, vol. 16, pp. 216-224.

[36] H. Konishi, T. Bitoh, H. Ono, T. Oishi, K. Koyama, and M. Tanaka: *Journal of JSEM*, 2014, vol. 14, pp. 205-209.

[37] Z. Sun, Y. Xiao, J. Sietsma, H. Agterhuis, and Y. Yang, Y. *Environ. Sci. Technol.*, 2015, vol. 49, pp. 7981-7988.

[38] B. Ghosh, M.K. Ghosh, P. Parhi, P.S. Mukherjee, and B.K. Mishra: *J. Cleaner Prod.*, 2015, vol. 94, pp. 5-19.

[39] E. Rudnik: *Arch. Metall. Mater.*, 2017, vol. 62, pp. 1681-1688.

[40] G.M. Gill, E. Ineson, and G.W. Austin: *J. Iron Steel Inst.*, 1959, vol. 191, pp. 172-175.

[41] M. Ollette: *Inst. de Recherches de Siderurgié*, 1961, vol. 111.

[42] R.G. Ward: *J. Iron & Steel Inst.*, 1963, pp. 11-15.

[43] E.T. Turkdogan, P. Grieveson, and L.S. Darken: *The Journal of Physical Chemistry*, 1963, vol. 67, pp. 1647-1654.

[44] W.A. Fischer,and M. Derenbach: *Archiv für das Eisenhüttenwesen*, 1964, vol. 35, pp. 307-316.

[45] P.N. Smith, and R.G. Ward: *Canadian Metallurgical Quarterly*, 1966, vol. 5, pp. 77-92.

[46] R. Ohno, and T. Ishida: *Science reports of the Research Institutes, Tohoku University. Ser. A*, 1968, vol. 21, pp. 130.

[47] W.A. Fischer, D. Janke, and K. Stahlschmidt: *Archiv für das Eisenhüttenwesen*, 1974, vol. 45, pp. 361-365.

[48] H. Salomon-de-Friedberg, and W.G. Davenport: *Can. Metall. Q.*, 1977, vol. 16, pp. 225-231.

[49] O. Reiichi: *Science reports of the Research Institutes, Tohoku University. Ser. A*, 1977, vol. 27, pp. 86-87.

[50] R. Harris, and W.G. Davenport: *Can. Metall. Q.*, 1979, vol. 18, pp. 303-311.

[51] M. Yamamoto, and E. Kato: *Tetsu-to-Hagané*, 1980, vol. 66, pp. 608-617.

[52] R. Harris: *McGill University,* PhD dissertation, 1979.

[53] D. Morales: *Ironmaking Steelmaking*, 1982, vol. 9, pp. 64-76.

[54] R. Harris, and W.G. Davenport: *J. Electron. Mater.*, 1982, vol. 21, pp. 581-588.

[55] R. Harris, and W.G. Davenport: *U.S. Patent No. 4,456,479*, 1983.

[56] R. Harris: *Can. Metall. Q.*, 1988, vol. 27, pp. 169-178.

[57] Matsuo: *Trans. Iron Steel Inst. Japan*, 1988, vol. 28, pp. 319.

[58] Y. Nakajima, T. Okimura, and J. Hirama, J: *ISIJ, Tokyo,* 1993.

[59] M. Hino, S.B. Wang, T. Nagasaka, and S. Ban-Ya: *Tetsu-to-Hagane*, 1994, vol. 80, pp. 300-305.

[60] T. Emi, and O. Wijk: *Iron and Steel Society, Warrendale, PA*, 1996.

[61] T. Matsuo, K. Maya, T. Nishi, K. Shinme, A. Ueno, and S. Anezaki: *ISIJ international*, 1996, vol. 36, pp. 62-65.

[62] H.S. Lee, and R. Harris: *The Canadian Journal of Chemical Engineering*, 1997, vol. 75, pp. 256-263.

[63] T. Nishi, S. Fukagawa, K. Shinme, and T. Matsuo: *ISIJ international*, 1999, vol. 39, pp. 905-912.

[64] A.I. Zaitsev, N.Y.E.E. Shelkova, A.D. Litvina, E.K. Shakhpazov, and B.M. Mogutnov: *High Temp.*, 1999, vol 39, pp. 388-394.

[65] Z. Ma, L. Savov, and D. Janke, D: *Metall*, 1999, vol. 53, pp. 61-67.

[66] L. Savov, and D. Janke: *ISIJ Int.* 2000, vol 40, pp. 95-104.

[67] T. Matsuo: *Tetsu-to-hagane*, 2000, vol. 86, pp. 741-747.

[68] H. Ono-Nakazato, K. Taguchi, Y. Seike, and T. Usui: *ISIJ Int.*, 2003, vol. 43, pp. 1691-1697.

[69] K. Taguchi, H. Ono-Nakazato and T. Usui: *Resources Processing*, 2004, vol. 51, pp. 158-162.

[70] A.I. Zaitsev, N.E. Zaitseva, E.K. Shakhpazov, and B.M. Mogutnov: *ISIJ Int.*, 2004, vol. 44, pp. 639-646.

[71] A.I. Zaitsev, N.E. Zaitseva, E.K. Shakhpazov, and B.M. Mogutnov: *ISIJ Int.*, 2004, vol. 44, pp. 957-964.

[72] N.A. Warner: *Metall. Mater. Trans. B*, 2004, vol. 35, pp. 663-674.

[73] L. Blacha, and J. Łabaj: *Science and Engineering*, 2011, vol. *51*, pp. 103-106.

[74] J. Łabaj, B. Oleksiak, and G. Siwiec: *Metalurgija*, 2011, vol. 50, pp. 265-268.

[75] L. Blacha, and J. Labaj: *Metalurgija/Metallurgy*, 2012, *51*(4), 529-533.

[76] S.H. Jung, and Y.B. Kang: *Metall. Mater. Trans. B*, 2016, vol. 47, pp. 2164-2176.

[77] S.H. Jung, and Y.B. Kang: *Metall. Mater. Trans. B*, 2016, vol. 47, pp. 2564-2570.

[78] O.N. Carlson and F.A. Schmidt: 103rd Annual AIME Meeting, Dallas, Texas, Feb 24-27, 1974.

[79] R.J. Andreini, and J.S. Foster: *J. of Vac. Sci. Technol*, 1974, vol. 11, pp. 1055-1059.

[80] H. Scholz, U. Biebricher, H. Franz, A. Paderni, and P. Bettoni: State of the art in VAR and ESR processes - a comparison (ASO Group Steel). http://www.asogroupsteel.com/wp-content/uploads/2014/05/var-and-esr-processes.pdf

[81] E.T. Turkdogan, P. Grieveson, and L.S. Darken: *J. Phys. Chem.*, 1963, vol. 67, pp. 1647-1654.

[82] T. Hidani, K. Takemura, R.O. Suzuki, and K. Ono: *Tetsu-to-Hagané*, 1996, vol. 82, pp. 135-140.

[83] L. Liansheng, L. Shiqi, X. Changxiang, C. Jie, L. Keming, and L. Suqin: *J. Iron Steel Res. Int.,* 1999, vol. 6, pp. 10-13.

[84] R.O. Suzuki, and K. Ono: *Proceedings of 10th International Conference on High Temperature Materials Chemistry,* 2000, pp. 491-494.

[85] T. Maruyama, H.G. Katayama, T. Momono, Y. Tayu, and T. Takenouchi: *Tetsu-to-Hagane*, 1998, vol. 84, pp. 243-248.

[86] L. Li, C.X. Xiang, J. Cao, S.Q. Li, and E.J. Ichise: *Journal of University of Science and Technology Beijing,* 1998, vol. 5, pp. 93-96.

[87] S. Li, B. Yu, S. Li, and L. Li: *Journal of Baotou University of Iron and Steel Technology,* 1999, 03.

[88] M. Sasabe, E. Harada, and S. Yamashita: *Tetsu-to-Hagané*, 1996, vol. 82, pp. 129-134.

[89] Y. Yuan, K. Sassa, K. Iwai, Q. Wang, J. He, and S. Asai: *ISIJ Int*, 2008, vol. 48, pp. 901-905.

[90] Z.H.I. Sun, M. Guo, J. Vleugels, O. Van der Biest, and B. Blanpain: *Curr. Opin. Solid State Mater. Sci.,* 2012, vol. 16, pp. 254-267.

[91] M. Nakamoto, Y. Okumura, T. Tanaka, and T. Yamamoto: *Tetsu-to-Hagané*, 2014, vol. 100, pp. 761-768.

[92] Z. Xiao-Wei, A. Bai-Ling, H. De-Yang, Z. Lin, and W. En-Gang: *Acta Physica Sinica,* , 2016, vol. 65.

[93] K. Yamaguchi, H. Ono, T. Usui: *Mater. Trans.*, 2010, vol. 51, pp. 1222-1226.

[94] P. Harald: *U.S. Patent No. 1,562,472*, 1925.

[95] F.C. Langenberg, and R.W. Lindsay: *AIME TRANS,* 1954, vol. 200, pp. 967-968.

[96] H. Schenck and G. Perbix: *Arch. Eisenhuettenwes*., 1962, vol. 33, pp. 417-20.

[97] T. Imai and N. Sano: *Trans. ISIJ,* 1988, vol. 28, pp. 999-1005.

[98] K. Yamaguchi, and Y. Takeda: *Mater. Trans.*, 2003, vol. 44, pp. 2452-2455.

[99] K. Yamaguchi, H. Ono, and T. Usui: *Tetsu-to-Hagane,* 2010, vol. 96, pp. 531-535.

[100] K. Yamaguchi, and H. Ono: *ISIJ Int.,* 2012, vol. 52, pp. 18-25.

[101] K. Yamaguchi, H. Ono, and E. Takeuchi: *Tetsu-to-Hagane,* 2015, vol. 101, pp. 636-644.

[102] A.J. Rose: *University of Cambridge Ph.D. Dissertation,* 1981.

[103] H.V. Makar, B. Dunning, and H. Caldwell: *U.S. Dept of the Interior, Bureau of Mines,* 1968.

[104] H.V. Makar, and B.W. Dunning: *JOM*, 1969, vol. 21, pp. 19-22.

[105] A.A. Safiah and F.R. Sale: *J. Iron and Steel Inst*, 1972, pp. 52-56.

[106] H.V. Makar, and R.E. Brown: U*.S. Dept of the Interior, Bureau of Mines,* 1974.

[107] Y.A. Topkaya, W.K. Lu: *Electrochem. Soc.,* 1974, vol. 111.

[108] M.C. Van Hecke, and L.M. Fontainas: *U.S. Patent No. 4,451,289*, 1984.

[109] X. Liu, and J.H.E. Jeffes: *Ironmaking Steelmaking*, 1985, vol. 12, pp. 293-294.

[110] T. Okazaki and D. G. C. Robertson: *Ironmaking Steelmaking*, 1985, vol. 12, pp. 295.

[111] L.L. Oden, G.W. Elger: *U.S. Bureau of Mines*, 1987, Report 9139.

[112] X. Liu, and J.H.E. Jeffes*: Ironnaking & Steelmaking*, 1989, vol. 16, pp. 331-334.

[113] C. Wang, T. Nagasaka, M. Hino, and S. Ban-Ya: *ISIJ Int.,* 1991, vol. 31, pp. 1300-1308.

[114] C. Wang, T. Nagasaka, M. Hino, and S. Ban-Ya: *ISIJ Int.,* 1991, vol. 31, pp. 1309-1315.

[115] В. КАШИН, А. КАЦНЕЛЬСОН, А. ДАНИЛОВИЧ: Сталь, 1991, 7. p.15-18.

[116] R. Shimpo, O. Ogawa, Y. Fukaya, and T. Ishikawa: *Metall. Mater. Trans. B*, 1997, vol. 28, pp. 1029-1037.

[117] A. Cohen, and M. Blander: *Metall. Mater. Trans. B*, 1998, vol. 29, pp. 493-495.

[118] Y. Kostetsky, A. Troyansky, and M. Samborsky: *Metal*, 2014.

[119] A. Cohen: *Northwestern University, Ph.D. Dissertation,* 2005.

[120] K. Hui, W. JianJun, G. Shangxing, Z. Li, and L. Jie: *High Temp. Mater. Proc.*, 2009, vol. 28, pp. 67-72.

[121] Y.I. Uchida, A. Matsui, Y. Kishimoto, and Y. Miki: *ISIJ Int.*, 2015, vol. 55, pp. 1549-1557.

[122] M. Sasabe, E. Harada, and S. Yamashita, S: *Tetsu-to-Hagané*, 1996, vol. 82, pp. 129-134.

[123] X. Hu, Z. Yan, P. Jiang, L. Zhu, K. Chou, H. Matsuura, and F. Tsukihashi: *ISIJ Int.*, 2013, vol. 53, pp. 920-922.

[124] Shredder Guide – high speed machinery. (Recycling Today, 2001), https://www.recyclingtoday.com/article/shredder-guide----high-speed-machinery-/. Accessed January 2019.

[125] H. Lassesson: *Chalmers University of Technology*, Masters thesis, 2008.

[126] S. Das, T.R. Curlee, C.G. Rizy, and S.M. Schexnayder: *Resour., Cons. Recycl.*, 1995, vol. 14, pp. 265-284.

[127] A.D. Shulman: *U.S. Patent No. 7,886,915*, 2011

[128] Trommels. (Bianna Recycling, 2018) http://biannarecycling.com/en/trommel/. Accessed January 2019.

[129] Energy and Environmental Profile of the U.S. Chemical Industry (U.S. Department of Energy, 2000),

www1.eere.energy.gov/manufacturing/resources/chemicals/pdfs/profile_full.pdf. Accessed September 2019.

[130] E. Worrell, D. Phylipsen, D. Einstein and N. Martin, Energy Use and Energy Intensity of the U.S. Chemical Industry, (University of California Berkeley, 2000). www.energystar.gov/ia/business/industry/industrial_LBNL-44314.pdf. Accessed September 2019.

[131] M.F. Ashby: *Materials and the Environment – Eco-Informed Material Choice*, 2013, 2 ed., Butterworth-Heinemann.

[132] F. Memoli, C. Giavani, and E. Malfa: *Industrial Heating*, 2012, *80*(8), 59.

[133] H.J. Karimi, and M.H. Saidi: *J. Iron Steel Res., Int.*, 2010, vol. 17, pp. 12-17.

[134] W.H. Chen, Y.C. Chung, and J.L. Liu: *Int. Commun. Heat Mass Transfer*, 2005, vol. 32, pp. 695-706.

[135] Rotary Electric Vibrators (Cleveland Vibrator, 2018): https://www.clevelandvibrator.com/images/Documents/Full%20RE%20Manual.pdf. Accessed September 2018.

[136] W. Schmitz and D. Trauzeddel. The melting, holding and pouring process – energy and process-related aspects (Otto Junker): http://www.hossl.com/archivos/201605/articulo-junker.pdf?1. Accessed September 2018.

[137] Z. Adolf, and L. Socha: Secondary Metallurgy (Ostrava, 2016), http://katedry.fmmi.vsb.cz/Opory_FMMI_ENG/2_rocnik/MMT/Secondary%20Metallurgy.pdf. Accessed September 2018.

[138] Y. Zhang, P.V. Barr, and T.R. Meadowcroft, *Mineral Eng.*, 2008, vol. 21, pp. 178-189.

[139] J.W. Matousek: *JOM,* 2008, vol. 60, pp. 62-64.

[140] Tilting Rotary Furnace (Melting Solutions), https://www.aluminium-messe.com/local/php/productpdf.php?id=6527&ext=.pdf. Accessed September 2018.

[141] ICE Database (Circular Ecology, 2018), http://www.circularecology.com/embodied-energy-and-carbon-footprint-database.html#.W5Jf5i-ZOb9. Accessed September 2018.

[142] A. Ghosh: *Secondary Steelmaking: Principles and Applications*, CRC Press, Boca Raton, 2000.

[143] S. Sarna: Desulphurization of Hot Metal (ISPAT Guru, 2013) http://ispatguru.com/desulphurization-of-hot-metal/. Accessed September 2018.

[144] W.D. Cho and P. Fan: *US Patent 7,789,936*, 2010.

[145] Y. Sun, Y. Xiao, J. Sietsma, H. Agterhuis, and Y. Yang: *Environ. Sci. and Tech.*, 2015, vol. 49, pp. 7981-7988.

[146] J. Jung, and W. Keller: *Erzmetall*, 2016 vol. 69, pp. 108-118.

[147] Energy Consumption of Tanks and Vats (Spirax Sarco Limited, 2018), *http://www.spiraxsarco.com/Resources/Pages/Steam-Engineering-Tutorials/steam-engineering-principles-and-heat-transfer/energy-consumption-of-tanks-and-vats.aspx.* Accessed September 2018.

[148] Morales, R. D., and M. M. Hernandez. "Kinetic model of steel refining in a ladle furnace." (2015).

[149] O. Winkler, and R. Bakish: *Vacuum Metallurgy*, Elsevier, New York, 1971.

[150] K.W. Lange: *Int. Mater. Rev.*, 1988, vol. 33, pp. 53-89.

[151] V.A. Kuznetsov, and Y.L. Kats: *Metallurgist,* 2007, vol. 51, pp. 220-225.

[152] Burgmann, W., & Göhler, K.: *Metallurgist*, 2013, vol. 57, pp. 516-525.

[153] B.M. Michaelis, D. Dunn-Rankin, R.F. Smith Jr, and J.E. Bobrow: *Int. J. Heat Mass Trans.*, 2007, vol. 50, pp. 4554-4558.

[154] M.A. Tayeb, S. Spooner, and S. Sridhar: *JOM*, 2014, vol. 66, pp.1565-1571.

[155] C. Bodsworth: *Physical chemistry of iron and steel manufacture,* 1963. Longmans.

[156] S.H. Kim, and R.J. Fruehan: *Metall. Mater. Trans. B*, 1987, vol. 18, pp. 381-390.

[157] E.S. Machlin: Trans. TMS-AIME, 1960, vol. 218, pp. 314-26.

[158] Y.Y. Sheng, and G.A. Irons: *Metall. Trans.,* 1992, vol. 23B, p. 779.

[159] E. Ramström: *Mass transfer and slag-metal reaction in ladle refining – a CFD approach*. KTH, Stockholm, 2010.

[160] T.A. Engh: *Principles of Metal Refining*, Oxford University Press, Oxford, 1992.

[161] J. Alexis, P. Jönsson, and L. Jonsson: *ISIJ Int.,* 2000, vol. 40, pp. 1098-1104.

[162] A. Thrum, Induction or gas stirring in ladle furnaces – a comparison. ABB Process Industries. http://www02.abb.com/GLOBAL/SEITP/seitp161.nsf/viewunid/83EE00B7C0AAB4D4C1256BF1004E41F8/$file/Induction+or+Gas+Stirring+in+Ladle+Furnaces.pdf. Accessed September 2018.

[163] J. Madias: *Treatise on Process Metallurgy: Industrial Processes*, 2014, pp. 271-300.

[164] National Bureau of Statistics of the People's Republic of China: *China Energy Statistical Yearbook 2013*, China Statistics Press: Beijing, China, 2013.

[165] M. Krüger, M. Reuter, C. Kögler, T. Probst: *Metallurgical Furnaces (Chap. 5),* Wiley, Weinheim 2005.

[166] R. Yin: *Metallurgical Process Engineering*, Metallurgical Industry Press, Beijing, 2009.